AMERICAN SOCIETY FOR MICROBIOLOGY | mSphere

Editor's Pick | Host-Microbial Interactions | Research Article

# PERK-mediated antioxidant response is key for pathogen persistence in ticks

**Kristin L. Rosche,[1] Joanna Hurtado,[1,2] Elis A. Fisk,[1] Kaylee A. Vosbigian,[1] Ashley L. Warren,[1] Lindsay C. Sidak-Loftis,[1] Sarah J. Wright,[1] Elisabeth Ramirez-Zepp,[1] Jason M. Park,[1] Dana K. Shaw[1,2]**

**AUTHOR AFFILIATIONS** See affiliation list on p. 16.

**ABSTRACT** A crucial phase in the life cycle of tick-borne pathogens is the time spent colonizing and persisting within the arthropod. Tick immunity is emerging as a key force shaping how transmissible pathogens interact with the vector. How pathogens remain in the tick despite immunological pressure remains unknown. In persistently infected *Ixodes scapularis*, we found that *Borrelia burgdorferi* (causative agent of Lyme disease) and *Anaplasma phagocytophilum* (causative agent of granulocytic anaplasmosis) activate a cellular stress pathway mediated by the endoplasmic reticulum receptor PKR-like ER kinase (PERK) and the central regulatory molecule eIF2α. Disabling the PERK pathway through pharmacological inhibition and RNA interference (RNAi) significantly decreased microbial numbers. *In vivo* RNAi of the PERK pathway not only reduced the number of *A. phagocytophilum* and *B. burgdorferi* colonizing larvae after a bloodmeal but also significantly reduced the number of bacteria that survive the molt. An investigation into PERK pathway-regulated targets revealed that *A. phagocytophilum* and *B. burgdorferi* induce activity of the antioxidant response regulator, nuclear factor erythroid 2-related factor 2 (Nrf2). Tick cells deficient for *nrf2* expression or PERK signaling showed accumulation of reactive oxygen and nitrogen species in addition to reduced microbial survival. Supplementation with antioxidants rescued the microbicidal phenotype caused by blocking the PERK pathway. Altogether, our study demonstrates that the *Ixodes* PERK pathway is activated by transmissible microbes and facilitates persistence in the arthropod by potentiating an Nrf2-regulated antioxidant environment.

**IMPORTANCE** Recent advances demonstrate that the tick immune system recognizes and limits the pathogens they transmit. Innate immune mediators such as antimicrobial peptides and reactive oxygen/nitrogen species are produced and restrict microbial survival. It is currently unclear how pathogens remain in the tick, despite this immune assault. We found that an antioxidant response controlled by the PERK branch of the unfolded protein response is activated in ticks that are persistently infected with *Borrelia burgdorferi* (Lyme disease) or *Anaplasma phagocytophilum* (granulocytic anaplasmosis). The PERK pathway induces the antioxidant response transcription factor, Nrf2, which coordinates a gene network that ultimately neutralizes reactive oxygen and nitrogen species. Interfering with this signaling cascade in ticks causes a significant decline in pathogen numbers. Given that innate immune products can cause collateral damage to host tissues, we speculate that this is an arthropod-driven response aimed at minimizing damage to "self" that also inadvertently benefits the pathogen. Collectively, our findings shed light on the mechanistic push and pull between tick immunity and pathogen persistence within the arthropod vector.

**KEYWORDS** *Ixodes scapularis*, *Borrelia burgdorferi*, *Anaplasma phagocytophilum*, tick-borne disease, vector competence, antioxidant response, PERK, eIF2α, ATF4, Nrf2

**Editor** Sarah E. F. D'Orazio, University of Kentucky College of Medicine, Lexington, Kentucky, USA

Address correspondence to Dana K. Shaw, dana.shaw@wsu.edu.

The authors declare no conflict of interest.

See the funding table on p. 16.

**Received** 14 June 2023
**Accepted** 31 July 2023
**Published** 21 September 2023

Ticks are prolific spreaders of pathogens that plague human and animal health (1), including bacteria, viruses, and protozoan parasites (2–4). A crucial phase in the tick-borne pathogen life cycle is the time spent colonizing and persisting within the arthropod vector (5). While many forces impact the way transmissible pathogens interface with their arthropod vectors, recent advances have demonstrated that tick immunity is an important influence shaping this interaction. Immune functions that respond to tick-transmitted bacterial pathogens include cellular defenses, such as phagocytosis by hemocytes, and humoral defenses orchestrated by immune deficiency (IMD) and Janus kinase-signal transducer and activator of transcription pathways (6–17). Notably, the tick IMD pathway is divergent from what has canonically been described in *Drosophila*. Ticks and other non-insect arthropods lack genes encoding key molecules, such as transmembrane peptidoglycan recognition proteins that initiate the IMD pathway, and the signaling molecules *IMD* and *FADD* (10, 18, 19) Instead, the tick IMD pathway responds to multiple cues such as infection-derived lipids that are sensed by the receptor Croquemort (10, 11, 17) and to cellular stress that is caused by infection (20, 21).

Recently, the unfolded protein response (UPR) has been linked to arthropod immunity (20). The UPR is a specialized cellular response pathway that is activated when the endoplasmic reticulum (ER) is under stress (22–24). Three ER receptors orchestrate the UPR and function to restore cellular homeostasis: activating transcription factor 6 (ATF6), PKR-like ER kinase (PERK), and inositol-requiring enzyme 1α (IRE1α). When *Ixodes scapularis* ticks are colonized by *Borrelia burgdorferi* (causative agent of Lyme disease) or *Anaplasma phagocytophilum* (causative agent of granulocytic anaplasmosis), the IRE1α receptor undergoes self-phosphorylation and pairs with TNF receptor associated factor 2 (TRAF2) to activate the IMD pathway (20). During this process, reactive oxygen species (ROS) are also potentiated. This signaling network functionally restricts the number of *Borrelia* and *Anaplasma* that colonize the tick (20). Furthermore, the UPR-IMD pathway connection and its pathogen-restricting potential are present in several arthropods against multiple types of pathogens, suggesting that this signaling network may be an ancient mode of pathogen sensing and vector defense against infection (20).

As vector immunity continues to be explored, a fundamental question has emerged: how are tick-borne pathogens persisting in the arthropod despite immunological pressure? Herein, we report that *B. burgdorferi* and *A. phagocytophilum* trigger phosphorylation of the central regulatory molecule, eIF2α, in *I. scapularis* ticks through the ER stress receptor PERK. Knocking down the PERK-eIF2α-ATF4 pathway *in vivo* through RNAi significantly inhibited *A. phagocytophilum* and *B. burgdorferi* colonization in ticks and reduced the number of microbes persisting through the molt. Infection-induced PERK pathway activation in *Ixodes* was connected to the antioxidant transcription factor, nuclear factor erythroid 2-related factor 2 (Nrf2). Disabling Nrf2 or the PERK pathway in tick cells caused accumulation of ROS and reactive nitrogen species (RNS) that led to greater microbial killing. This microbicidal phenotype could be rescued by exogenously supplementing antioxidants, demonstrating that the PERK pathway supports microbial persistence by detoxifying ROS/RNS. Overall, we have uncovered a mechanism at the vector-pathogen interface that promotes persistence of transmissible microbes in the arthropod despite active immune assaults.

## RESULTS

### Cellular stress genes are transcriptionally induced in infected, unfed *I. scapularis* nymphs

Infectious microbes impart cellular stress on the host (25). For this reason, we investigated whether cellular stress responses impact how microbes survive in ticks (20). We previously observed that the IRE1α-TRAF2 axis of the *I. scapularis* UPR responds to *A. phagocytophilum* and *B. burgdorferi* and functionally restricts pathogen colonization during a larval blood meal by crosstalking with the IMD pathway and potentiating ROS (Fig. 1A) (20). How *Anaplasma* and *Borrelia* persist in the tick despite this immunological

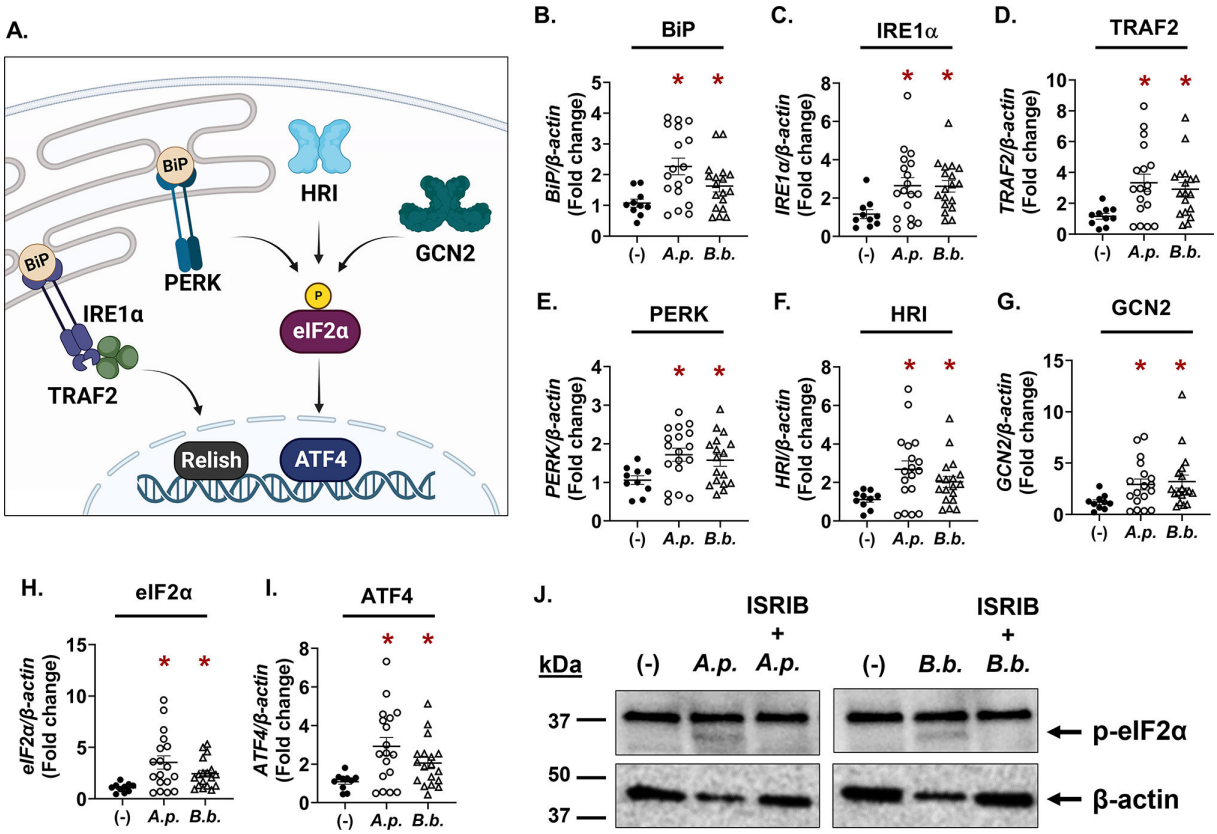


**FIG 1** Tick-borne pathogens induce eIF2α-regulated stress responses in infected, unfed nymphs. (A) Graphic representation of IRE1α-TRAF2 signaling and the integrated stress response pathways in *Ixodes* ticks. (B–I) Gene expression in flat, unfed *I. scapularis* nymphs that are either uninfected (–), *A. phagocytophilum*-infected (*A.p.*), or *B. burgdorferi*-infected (*B.b.*). Each data point is representative of one nymph. Gene expression was quantified by qRT-PCR using primers listed in Table S1. Student's *t*-test. *$P < 0.05$. (J) Phosphorylated eIF2α (36 kDa) immunoblot against ISE6 tick cells that were either uninfected (–), infected for 24 h (MOI 50), or treated with the eIF2α phosphorylation inhibitor ISRIB for 1 h prior to infection (24 h). β-Actin was probed as an internal loading control (45 kDa). Immunoblots are representative of two biological replicates. See also Fig. S1. *A.p.*, *A. phagocytophilum*; *B.b.*, *B. burgdorferi*; ISRIB, integrated stress response inhibitor.

pressure is not well understood. In this study, we analyzed the transcriptional response of *I. scapularis* nymphs that were infected but were unfed (flat) to explore how ticks respond to persistent infection. We found that, similar to results from immediately repleted ticks (20), unfed nymphs that are infected with *A. phagocytophilum* or *B. burgdorferi* showed increased expression of genes associated with IRE1α-TRAF2 signaling (Fig. 1B through D). In addition, we also found increased expression of genes that are part of the PERK pathway and another cellular stress response network termed the "integrated stress response" (ISR) (Fig. 1E through I).

The ISR is a highly conserved signaling network that is activated by cellular stress in eukaryotes (26, 27). Four different stress-sensing kinases initiate the ISR in mammals: general control non-derepressible (GCN2), heme-regulated inhibitor (HRI), protein kinase double-stranded RNA-dependent (PKR), and PERK, which is also part of the UPR network (28, 29). eIF2α is the central regulatory molecule that all ISR kinases converge on, which then activates the transcription factor ATF4 (Fig. 1A). ATF4 can also act as a transcriptional repressor of genes that lead to cell death (30, 31). Although the ISR is much less studied in arthropods relative to mammals, genome analysis demonstrates that ticks encode most ISR components with the exception of a PKR ortholog (18, 21). We found that *B. burgdorferi* or *A. phagocytophilum* infection transcriptionally induced the ISR kinases (*PERK*, *GCN2*, and *HRI*), the *eIF2α* regulatory molecule, and *ATF4* in flat, unfed nymphs (Fig. 1E through I).

ISR activation can be monitored by probing for the phosphorylation status of eIF2α (26, 29). When eIF2α amino acid sequences from human and *I. scapularis* were aligned, we observed a good amount of sequence similarity (70.71% identity, Fig. S1A). Importantly, the activating residue that is phosphorylated by ISR kinases, Ser51, is conserved. We therefore used a commercially raised antibody specific for phosphorylated eIF2α to monitor ISR activation in tick cells. Relative to non-treated controls, ISE6 cells infected with either *A. phagocytophilum* or *B. burgdorferi* showed a band at approximately 36 kDa, correlating with the predicted molecular weight of *I. scapularis* eIF2α (Fig. 1J, band indicated with black arrow). When tick cells were treated with a small molecule inhibitor of eIF2α phosphorylation, integrated stress response inhibitor (ISRIB) (32), the 36 kDa band was no longer present, indicating that the band observed was specific to phosphorylated eIF2α (Fig. 1J). Altogether, these data show that cellular stress responses converging on eIF2α are activated by *A. phagocytophilum* and *B. burgdorferi* in ticks.

## The PERK pathway promotes *A. phagocytophilum* growth and survival in tick cells

To determine how eIF2α-regulated stress responses impact pathogen survival in ticks, pharmacological modulators or RNAi silencing were used in *I. scapularis* cells. ISRIB inhibits phosphorylation of eIF2α (32), thereby shutting down the ISR. In contrast, salubrinal is an eIF2α activator and promotes ISR activity (33, 34). We observed that each pharmacological modulator had opposing effects on *A. phagocytophilum* colonization and replication. Inhibiting eIF2α with ISRIB caused a dose-dependent decline in bacteria (Fig. 2A). In contrast, promoting eIF2α activation with salubrinal conferred a survival advantage (Fig. 2B). We next used an RNAi-based knockdown approach targeting either *eIF2α* or the downstream transcription factor, *ATF4*. In agreement with pharmacological inhibition, transcriptional silencing caused a decline in *A. phagocytophilum* numbers (Fig. 2C and D), indicating that eIF2α-regulated stress responses promote pathogen survival in tick cells.

We next sought to determine which upstream stress-sensing kinase is involved during infection. RNAi knockdown was used to silence the expression of *HRI*, *GCN2*, and *PERK* in tick cells. Although significant silencing was observed for each treatment (Fig. 2E and F), a defect in *A. phagocytophilum* survival was only observed with *PERK* knockdown (Fig. 2G). This survival defect correlated with what was observed when *eIF2α* and *ATF4* were silenced (Fig. 2C and D) or pharmacologically inhibited by ISRIB (Fig. 2A), suggesting that PERK may be the activating kinase.

## Pathogen colonization and persistence in ticks is supported by PERK, eIF2α, and ATF4

To determine whether the pro-survival role of the PERK pathway observed *in vitro* had a similar impact on microbes *in vivo*, we used RNAi in *I. scapularis* larvae together with *Anaplasma* or *Borrelia*. Distinct tissue tropisms and kinetics are exhibited in ticks by the intracellular rickettsial bacterium, *A. phagocytophilum*, and the extracellular spirochete, *B. burgdorferi*. *A. phagocytophilum* enters the midgut with a blood meal and rapidly traverses the midgut epithelium to colonize the salivary glands (7, 35, 36). In contrast, *B. burgdorferi* remains in the midgut during the molt and colonizes the tick between the midgut epithelium and peritrophic membrane (37, 38). Owing to these differences, we evaluated how *Ixodes* PERK signaling impacts colonization and persistence of both pathogens. An overnight small interfering RNA (siRNA) immersion protocol (20) was used to silence *PERK*, *eIF2α*, or *ATF4* in *I. scapularis* larvae. The next day, larvae were dried and rested before being placed on infected mice. With this approach, we observed significant knockdown of targeted genes (Fig. 3A, E, and I; Fig. 4A E, and I).

After ticks fed to repletion, pathogen numbers were quantified at three different time points that correspond to (i) pathogen acquisition (immediately after repletion), (ii) population expansion in the tick [7–14 days post-repletion (39)], and (iii) pathogen persistence through the molt (4–6 weeks post-repletion). Ticks evaluated immediately

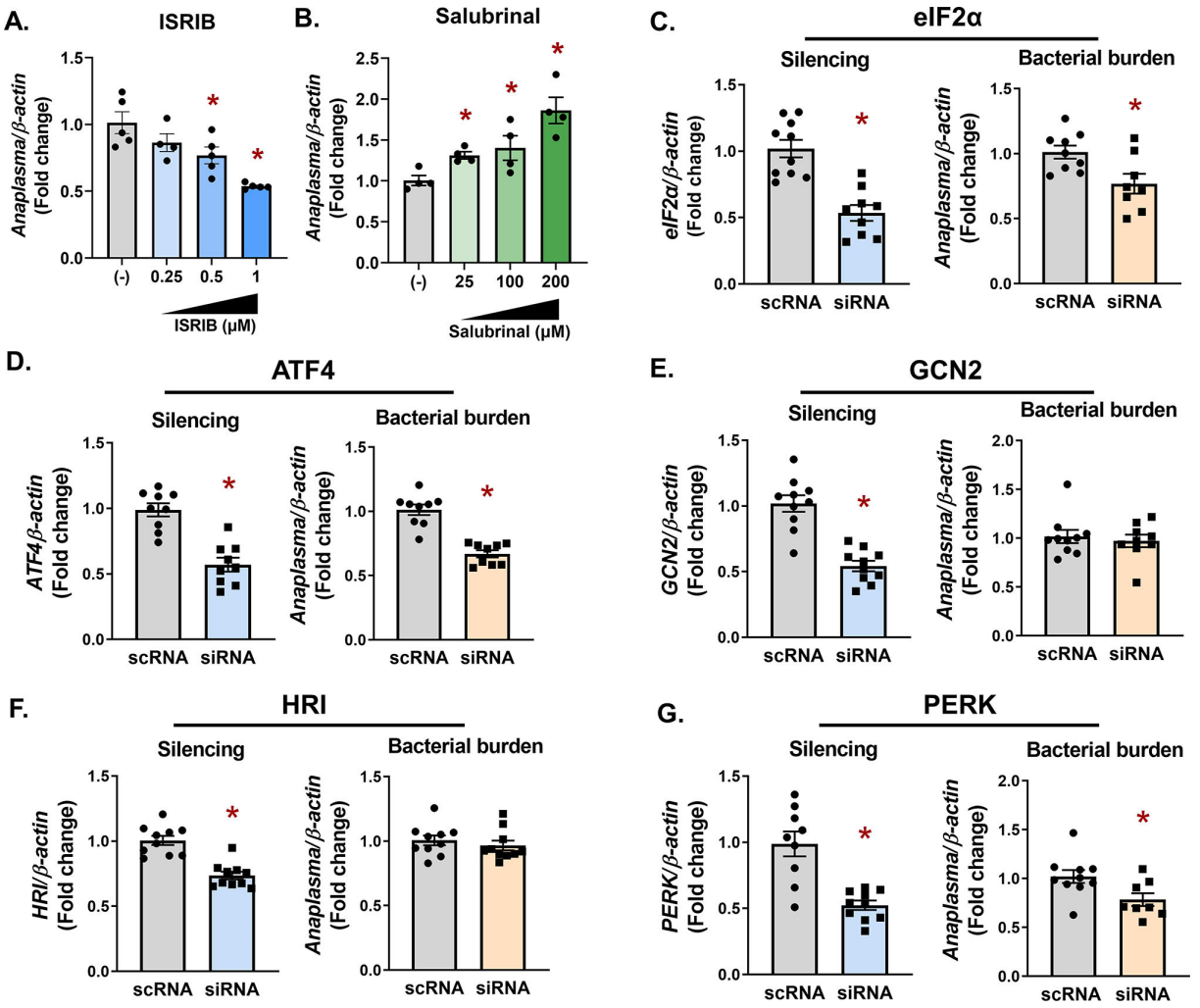


**FIG 2** The PERK-eIF2α-ATF4 axis promotes *A. phagocytophilum* infection in tick cells. (A and B) ISE6 tick cells ($1 \times 10^6$) were pretreated with ISRIB (A) or salubrinal (B) at the indicated concentrations for 1 h prior to infection with *A. phagocytophilum* for 18 h (MOI 50). (C–G) IDE12 tick cells ($1 \times 10^6$) were treated with silencing RNAs (siRNAS) against indicated genes or scRNA controls for 24 h prior to infection with *A. phagocytophilum* (MOI 50) for 18 h. *A. phagocytophilum* burden and gene silencing for *eIF2α* (C), *ATF4* (D), *GCN2* (E), *HRI* (F), and *PERK* (G) were measured by qRT-PCR. Data are representative of at least five biological replicates with at least two technical replicates. Error bars show standard error of the mean. **P* < 0.05 (Student's *t*-test). scRNA, scrambled RNA; siRNA, small interfering RNA.

after repletion (Fig. 3B, F, and J) and 7 days post-repletion (Fig. 3C, G, and K) showed a 2–6× reduction in *Anaplasma* numbers, indicating that the PERK-eIF2α-ATF4 pathway has a pro-survival role *in vivo*. However, ticks silenced for *PERK*, *eIF2α* or *ATF4* as larvae did not show statistically significant differences in *Anaplasma* burden as nymphs (Fig. 3D, H, and L). This may be due to the loss of transcriptional knockdown over the duration of the molt (4–6 weeks) or pathogen numbers rebounding after escaping the midgut to the salivary glands. For *Borrelia*, knocking down *PERK*, *eIF2α*, and *ATF4* (Fig. 4A, E, and I) also caused a 2–10× decrease in bacterial numbers at early colonization time points (Fig. 4B, C, F, G, J, and K). However, in contrast to *Anaplasma*, *Borrelia* remained significantly decreased after replete larvae molted to nymphs (Fig. 4D, H, and L). It is not clear why *Borrelia* remained restricted after the molt, while *Anaplasma* did not. A possible explanation could be a difference in microbial proliferation between *Anaplasma* and *Borrelia*. Another possibility is the fundamental difference in tick colonization sites, as the midgut is generally a more hostile environment for invading microbes than the salivary glands (40, 41). Taken as a whole, these data indicate that the *Ixodes* PERK pathway supports both extracellular and intracellular tick-borne microbes *in vivo*.

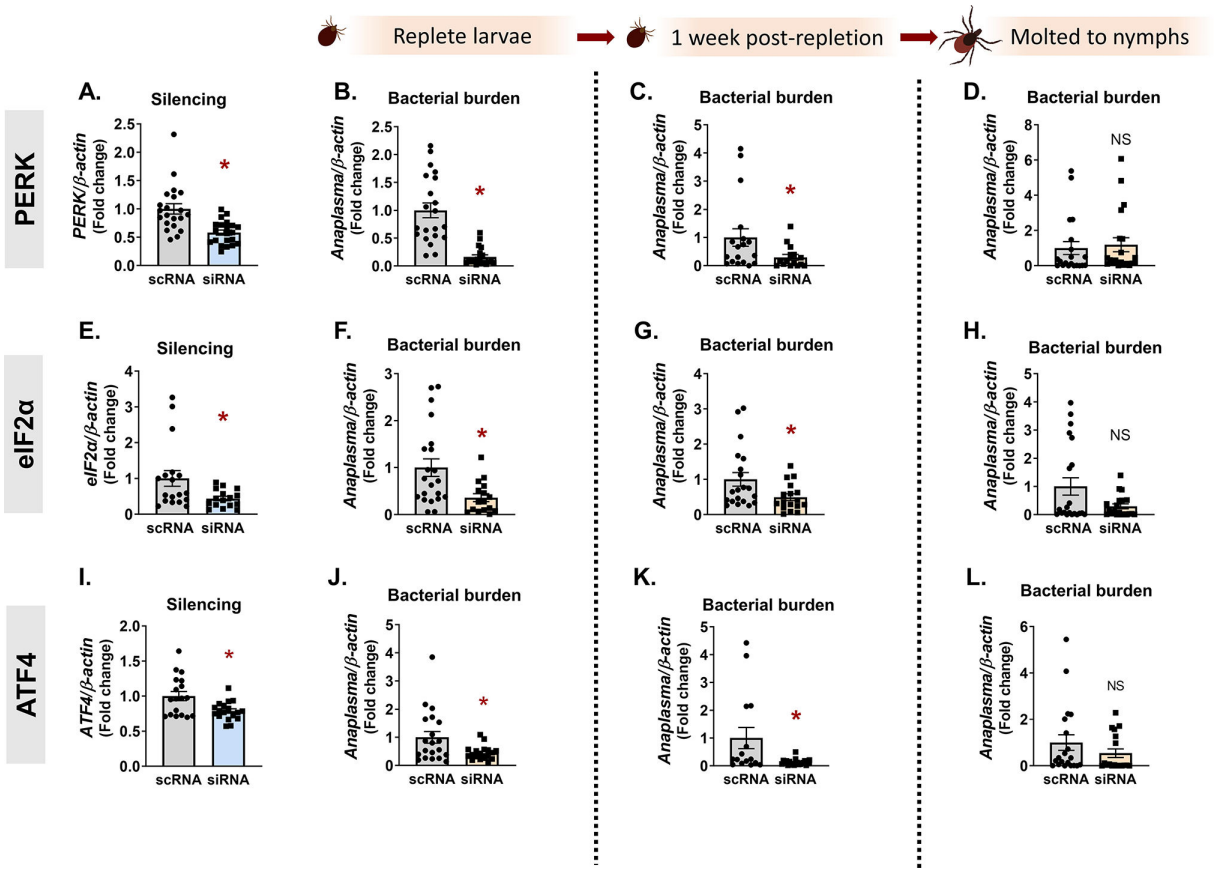


**FIG 3** The PERK pathway supports *A. phagocytophilum in vivo*. *I. scapularis* larvae were immersed overnight in siRNA targeting *PERK* (A–D), *eIF2α* (E–H), or *ATF4* (I–L) and fed on *A. phagocytophilum*-infected mice. Silencing efficiency (A, E, and I) and bacterial burden were assessed at three time intervals by qRT-PCR: immediately following repletion (B, F, and J), 1 week post-repletion (C, G, and K), and after ticks molted to nymphs (D, H, and L). Data are representative of 10–20 ticks and at least two experimental replicates. Each point represents one tick, with two technical replicates. Error bars show standard error of the mean. *$P < 0.05$ (Mann-Whitney test). NS, non-significant; scRNA, scrambled RNA, siRNA, small interfering RNA.

## *A. phagocytophilum* and *B. burgdorferi* trigger an Nrf2 antioxidant response in ticks

The microbe-supporting activity of the PERK-eIF2α-ATF4 pathway led us to ask what downstream signaling events occur that functionally promote pathogen survival. Genetic manipulation techniques in *I. scapularis* ticks and tick cell lines remain challenging. To circumvent this limitation, we employed a surrogate reporter system to interrogate downstream signaling events from the PERK pathway. A collection of luciferase reporter plasmids with promoter sequences for transcription factors associated with ER stress (XBP1, NF-κB, CHOP, SREBP1, and Nrf2) were transfected into HEK293 T cells. Transfected cells were then either infected with *A. phagocytophilum* or *B. burgdorferi* or left uninfected. After 24 h, luciferase activity was quantified to ascertain the transcriptional activity of each promoter (Fig. 5A and B). In agreement with previous reports (20), XBP1 activation was not observed with either *A. phagocytophilum* or *B. burgdorferi*. In contrast, the immunoregulatory transcription factor NF-κB was significantly induced by both, which is also in agreement with previous findings (42–45). Infection did not induce CHOP or SREBP1 activity but did robustly activate the antioxidant regulator Nrf2 (Fig. 5A and B).

Nrf2 is an evolutionarily conserved cap'n'collar transcription factor that coordinates antioxidant responses (49–53). It functions by binding to a consensus DNA sequence (antioxidant response elements (AREs)) in the promoter regions of Nrf2-regulated genes

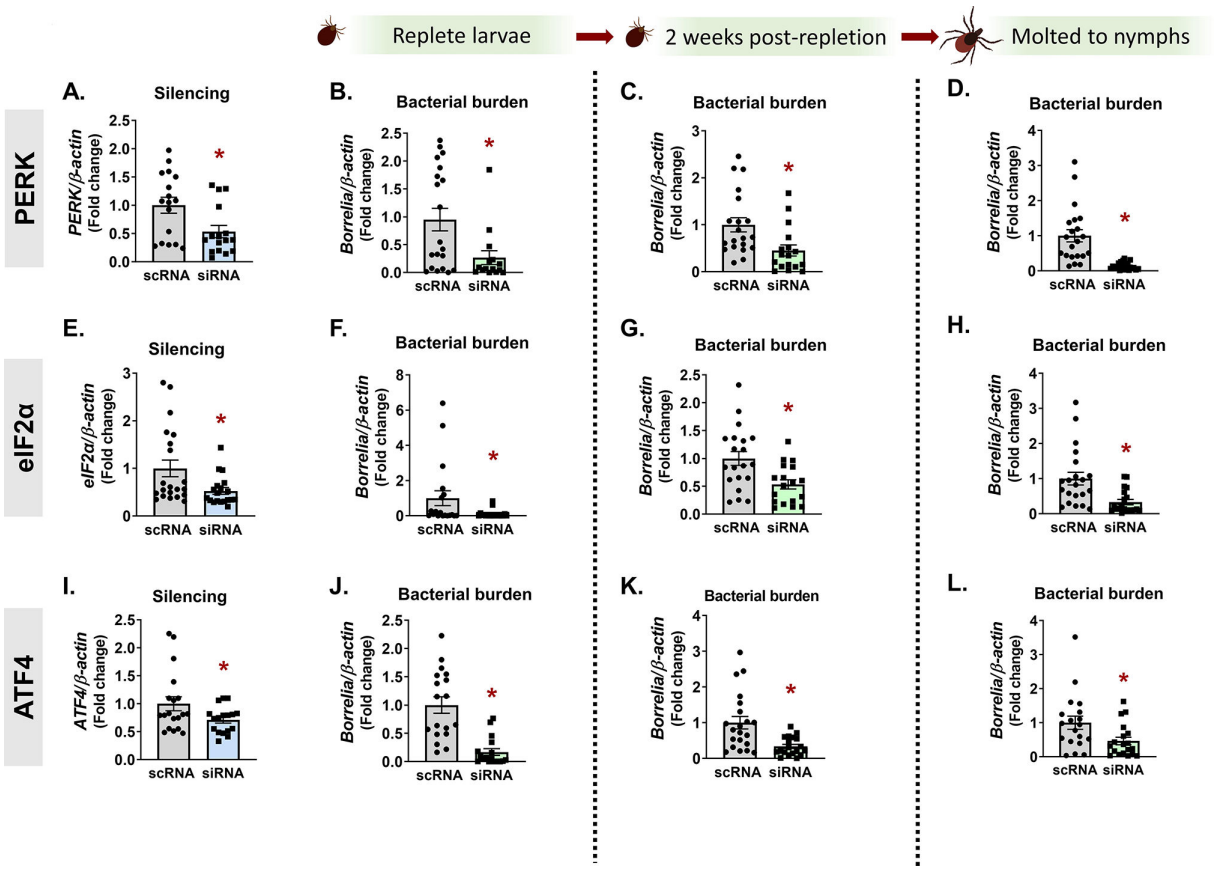


**FIG 4** *In vivo B. burgdorferi* colonization and persistence through the molt is supported by the PERK pathway. *PERK* (A–D), *eIF2α* (E–H), or *ATF4* (I–L) were silenced in *I. scapularis* larvae by immersing ticks in siRNA overnight. Recovered ticks were fed on *B. burgdorferi*-infected mice. Silencing efficiency (A, E, and I) and bacterial burden were assessed at three time intervals by qRT-PCR: immediately following repletion (B, F, and J), 2 weeks post-repletion (C, G, and K), and after ticks molted to nymphs (D, H, and L). Data are representative of 10–20 ticks and at least two experimental replicates. Each point represents one tick, with two technical replicates. Error bars show standard error of the mean. *$P < 0.05$ (Mann-Whitney test). scRNA, scrambled RNA, siRNA, small interfering RNA.

(54, 55). To identify an Nrf2 ortholog in *I. scapularis*, we used the human Nrf2 protein sequence to query the tick genome (56). A BLAST analysis returned the *Ixodes* protein XP_042149334.1. Although *I. scapularis* Nrf2 had low sequence conservation with human Nrf2 (45.67% identity, Fig. S2A), it did display a high degree of structural conservation when modeled with AlphaFold (Fig. 5C and D; *Ixodes* Nrf2—blue, Human Nrf2—orange; Fig. S2B). Notably, amino acids within the basic leucine zipper (bZIP) domain of Nrf2 that mediate DNA interactions with promoter ARE regions (57) were well conserved in the *Ixodes* protein (R877, R880, R882, N885, A888, A889, R893, R895, and K896; Fig. S2A; Fig. 5D).

To determine if *nrf2* transcriptionally responds to infection, we evaluated *nrf2* gene expression in flat, unfed nymphs. We observed significantly higher *nrf2* expression in nymphs infected with *A. phagocytophilum* and *B. burgdorferi* relative to uninfected controls (Fig. 5E). Since vertebrate Nrf2 regulates basal and inducible antioxidant genes, we next asked whether the *Ixodes* Nrf2 ortholog influences the tick cell redox environment. Tick cells were transfected with silencing RNAs against *nrf2* or with scrambled controls. Cells were then infected with *A. phagocytophilum* and ROS were measured with the fluorescent indicator 2′,7′-dichlorofluorescein diacetate (DCF-DA). We found that depleting *Ixodes nrf2* caused a significantly higher amount of ROS when compared to scrambled controls (Fig. 5F).

ROS is a potent antimicrobial agent, and it is well established that *A. phagocytophilum* and *B. burgdorferi* are sensitive to ROS-mediated killing (58–61). Considering Nrf2's role

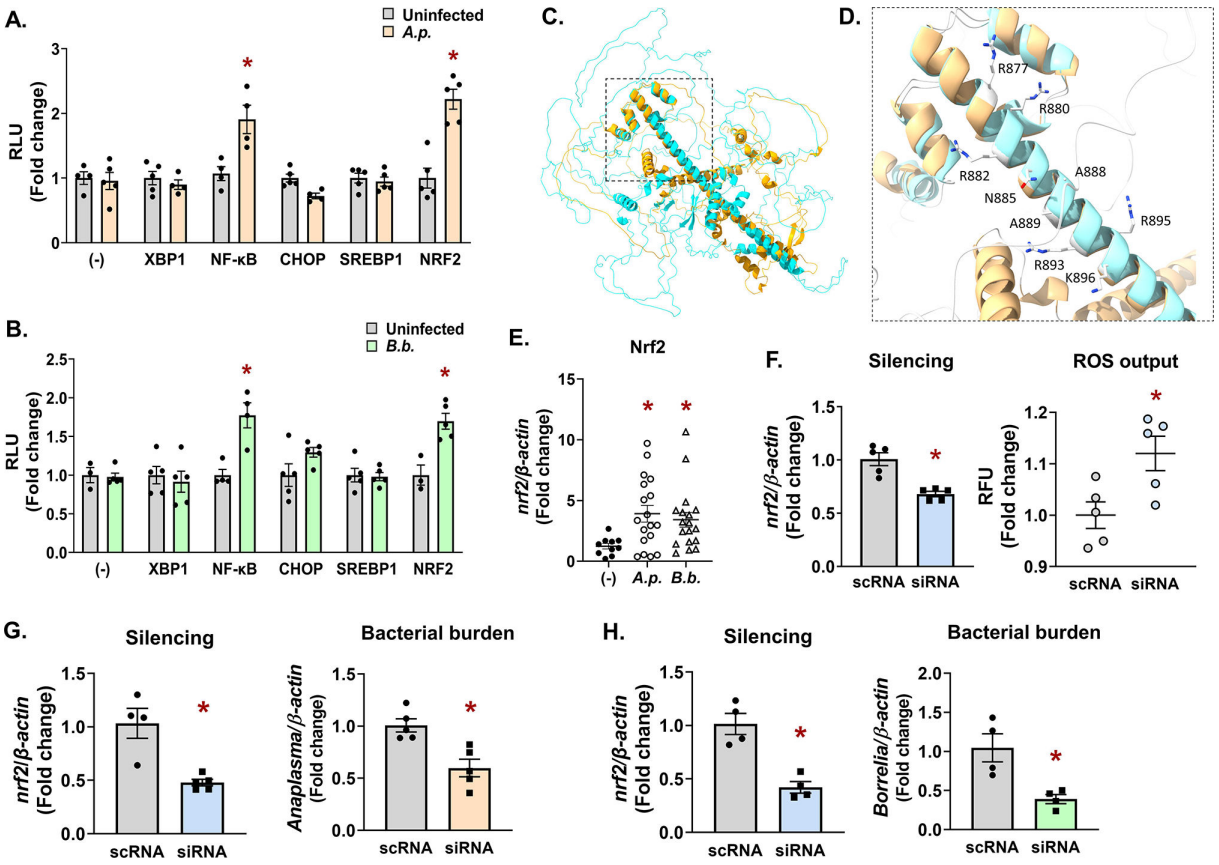


**FIG 5** Infection triggers an Nrf2-regulated antioxidant response in ticks that promotes pathogen survival. (A and B) HEK293T cells ($1 \times 10^4$) were transfected with luciferase reporter vectors for assaying activity of ER stress transcription factors XBP1, NF-κB, CHOP, SREBP1, and NRF2 or were untransfected (–). Cells were then infected with *A.p.* (A) or *B.b.* (B). After 24 h, D-luciferin was added and luminescence was measured as RLU. Measurements were normalized to uninfected controls (gray bars). Luciferase assays are representative of three to five biological replicates with at least two experimental replicates ± SEM. Student's *t*-test. **P* < 0.05. (C and D) Predicted *Ixodes* Nrf2 structure modeled with AlphaFold (46, 47) (blue) and overlaid with human Nrf2 (orange) using UCSF ChimeraX.(48) The bZIP domain is indicated by a box with dashed lines. (D) Magnified region of the bZIP domain depicting residues that that are predicted to interact with antioxidant response element sequences in DNA promoter regions (R877, R880, R882, N885, A888, A889, R893, R895, and K896). See also Fig. S2. (E) Nrf2 expression levels in flat, unfed nymphs that are uninfected (–), *A.p.*-infected, or *B.b.*-infected. Each data point is representative of one nymph. Gene expression was quantified by qRT-PCR using Nrf2 primers listed in Table S1. Student's *t*-test. **P* < 0.05. (F–H) IDE12 tick cells were treated with silencing RNAs (siRNA) targeting *nrf2* for 24 h prior to infection with *A. phagocytophilum* (18 h) (F and G) or *B. burgdorferi* (H). Gene silencing (F–H) and bacterial burden (G and H) were quantified by qRT-PCR. ROS was measured as relative fluorescent units after 24 h of infection (F). Data are representative of at least four to five biological replicates and two technical replicates. Error bars show SEM, **P* < 0.05 (Student's *t*-test). bZIP, basic leucine zipper; RLU, relative luminescence unit; scRNA, scrambled RNA; SEM, standard error of the mean; siRNA, small interfering RNA.

as an antioxidant regulator, we reasoned that silencing *nrf2* expression should enhance microbial killing owing to accumulated ROS. Accordingly, we found that when *nrf2* was knocked down in tick cells, there was a significant decline in *A. phagocytophilum* and *B. burgdorferi* survival (Fig. 5G and H). Collectively, these results support the conclusion that *Ixodes* Nrf2 is induced during infection and functionally promotes an antioxidant response, which confers a pro-survival environment for transmissible microbes in the tick.

## Antioxidant activity of the PERK-eIF2α pathway protects pathogen survival in tick cells

*A. phagocytophilum* and *B. burgdorferi* induce Nrf2, which is a transcriptional activator downstream from the PERK pathway (27). We therefore asked whether blocking eIF2α during infection would influence the redox environment in ticks. Tick cells were

either uninfected, infected (*A. phagocytophilum* or *B. burgdorferi*), or treated with the eIF2α inhibitor ISRIB prior to infection. Kinetic measurements of ROS and RNS were monitored in tick cells with the fluorescent reporters DCF-DA (ROS) or 4,5-diaminofluorescein diacetate (RNS) (Fig. 6A through D). In untreated cells, *A. phagocytophilum* infection caused a rise in ROS that peaked at 24 h. Thereafter, ROS levels declined, which is consistent with reports that *A. phagocytophilum* infection suppresses ROS (62–65). However, when eIF2α signaling is blocked with the ISRIB inhibitor, *A. phagocytophilum* caused increased ROS throughout infection that never declined (Fig. 6A; Fig. S3). Similarly, *B. burgdorferi* induced ROS in tick cells, and treating with ISRIB showed greater accumulation of ROS than infection alone (Fig. 6B; Fig. S3A). Inhibiting eIF2α had similar impacts on RNS in tick cells infected with *A. phagocytophilum* and *B. burgdorferi* (Fig. 6C and D; Fig. S3B). Combining ISRIB with infection conditions caused significantly higher RNS compared to infection alone. Unexpectedly, we also observed that untreated infection conditions showed a decline in RNS, which may suggest that *Anaplasma* and *Borrelia* suppress nitrosative stress in the tick. Collectively, these data indicate that eIF2α signaling functionally coordinates an antioxidant response in tick cells during infection.

We next asked if the antioxidant environment potentiated by the PERK-eIF2α-ATF4 pathway was the functional mechanism that supports pathogen survival in ticks. We first established that antioxidants enhance microbial survival in ticks. Tick cells that were supplemented with the antioxidant N-acetyl cysteine (NAC) during infection showed significantly more *A. phagocytophilum* or *B. burgdorferi* survival when compared to untreated controls (Fig. 6E and F). We then asked if the antioxidant activity of NAC could rescue the microbicidal phenotype caused by silencing *perk*. Tick cells were treated with silencing RNA against *perk* or scrambled controls, then infected with *A. phagocytophilum* or *B. burgdorferi* with and without NAC. We observed that silencing the expression of *perk* caused a rise is ROS (Fig. S4A and B) and a corresponding decrease in pathogen survival (Fig. 6G and H). However, supplementing with exogenous antioxidants neutralized the increased ROS caused by blocking the PERK pathway (Fig. S4A and B) and rescued bacterial survival (Fig. 6G and H). Altogether, our findings support a model where transmissible pathogens activate the PERK-eIF2α-ATF4 pathway, which functionally supports pathogen persistence in ticks through an Nrf2-mediated antioxidant response (Fig. 7).

## DISCUSSION

How pathogens persist in the tick is likely a multifaceted topic involving complex interactions orchestrated by both the microbe and the arthropod. In this article, we shed light on one aspect of this subject by demonstrating that *Anaplasma* and *Borrelia* infection activates the *Ixodes* PERK-eIF2α-ATF4 stress response pathway, which facilitates pathogen survival. The microbe-benefiting potential of this pathway was ultimately connected to an antioxidant response that is mediated by the *Ixodes* Nrf2 ortholog. Collectively, our findings have uncovered a piece of the puzzle in understanding how pathogens can persist in the tick despite immunological pressure from the arthropod vector.

*A. phagocytophilum* and *B. burgdorferi* have significantly different lifestyles (obligate intracellular vs extracellular) and tissue tropisms (salivary glands vs midgut), but both induce a state of oxidative stress upon tick colonization (20). Given that these microbes are susceptible to killing by oxidative and nitrosative stress (58, 60, 61, 65–73), it is perhaps not surprising that both would benefit from an antioxidant response in the tick. However, some discrepancies between *Anaplasma* and *Borrelia* survival phenotypes were observed at different time points *in vivo*. Bacterial colonization was decreased in larvae when *PERK*, *eIF2α*, or *ATF4* were knocked down by RNAi (Fig. 3 and 4). In contrast, *Borrelia* remained significantly reduced in molted nymphs, but *Anaplasma* numbers rebounded. This may be attributable to differences in tissue tropisms for each pathogen. *Anaplasma* rapidly escapes the midgut and colonizes the salivary glands (7, 35, 36), whereas *B. burgdorferi* remains in the midgut during the molt (37, 38). The midgut is a niche that is

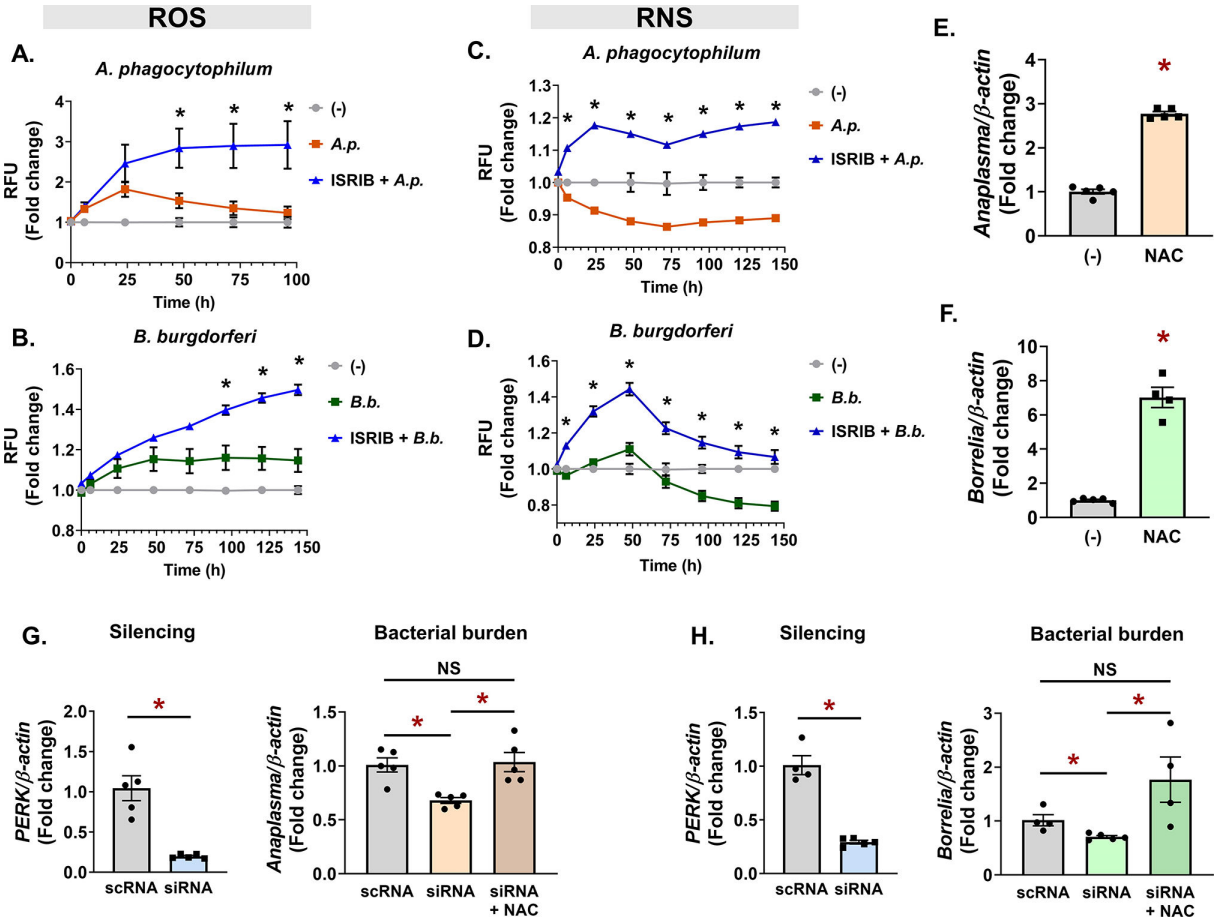


**FIG 6** Antioxidant activity of the PERK-eIF2α pathway protects pathogens in ticks. (A–D) ROS (A and B) and RNS (C and D) measurements in ISE6 cells ($1.68 \times 10^5$) untreated (-), infected (*A.p.* or *B.b.*), or pretreated with 1-μM ISRIB prior to infection with *A. phagocytophilum* (ISRIB + *A.p.*) (A and C) or *B. burgdorferi* (ISRIB + *B.b.*) (B and D). Fluorescence was measured at the indicated time points and is presented as RFU, normalized to untreated, uninfected controls (–). See also Fig. S3A and B. (E and F) IDE12 cells were infected with *A. phagocytophilum* (E) or *B. burgdorferi* (F) alone or in the presence of NAC for 24 h. (G and H) *perk* was silenced in IDE12 cells ($1 \times 10^6$). Cells were infected with *A. phagocytophilum* (G) or *B. burgdorferi* (H) alone or in the presence of NAC. See also Fig. S4A and B. Silencing levels and bacterial burdens were quantified by qRT-PCR. Data are representative of at least four to five biological replicates and two technical replicates. Error bars show SEM. **P* < 0.05 (Student's *t*-test). NAC, N-acetyl cysteine; RFU, relative fluorescent unit; scRNA, scrambled RNA; siRNA, small interfering RNA.

generally hostile to microbes owing to several factors including ROS and RNS production (40, 41, 68, 69) and may explain why *Borrelia* numbers are restricted even after larvae molt to nymphs. The *Ixodes* salivary gland environment also produces ROS and RNS (68), but antioxidant proteins found in salivary glands, such as the peroxiredoxin Salp25D (74), may protect *Anaplasma* and explain why pathogen numbers rebounded after the molt.

Since *A. phagocytophilum* and *B. burgdorferi* are susceptible to oxidative and nitrosative damage (58–61, 65, 67–71), these microbes may be inducing the *Ixodes* PERK-eIF2α-ATF4-Nrf2 pathway to create a more hospitable environment and facilitate persistence. *A. phagocytophilum* replicates intracellularly and secretes a suite of effectors that manipulate host cell biology and promote the formation of a replicative niche. Although only one tick-specific effector has been characterized to date (75), it is conceivable that *Anaplasma* manipulates PERK pathway activation in the tick with secreted effector molecules. *B. burgdorferi* replicates extracellularly and does not encode any secretion systems for effector transport, which makes direct host-cell manipulation less likely. However, it is possible that *Borrelia* may transport small molecules (67) that could activate the PERK pathway and promote an antioxidant response. Alternatively, the PERK-eIF2α-ATF4-Nrf2 signaling cascade may be responding to general stress signals

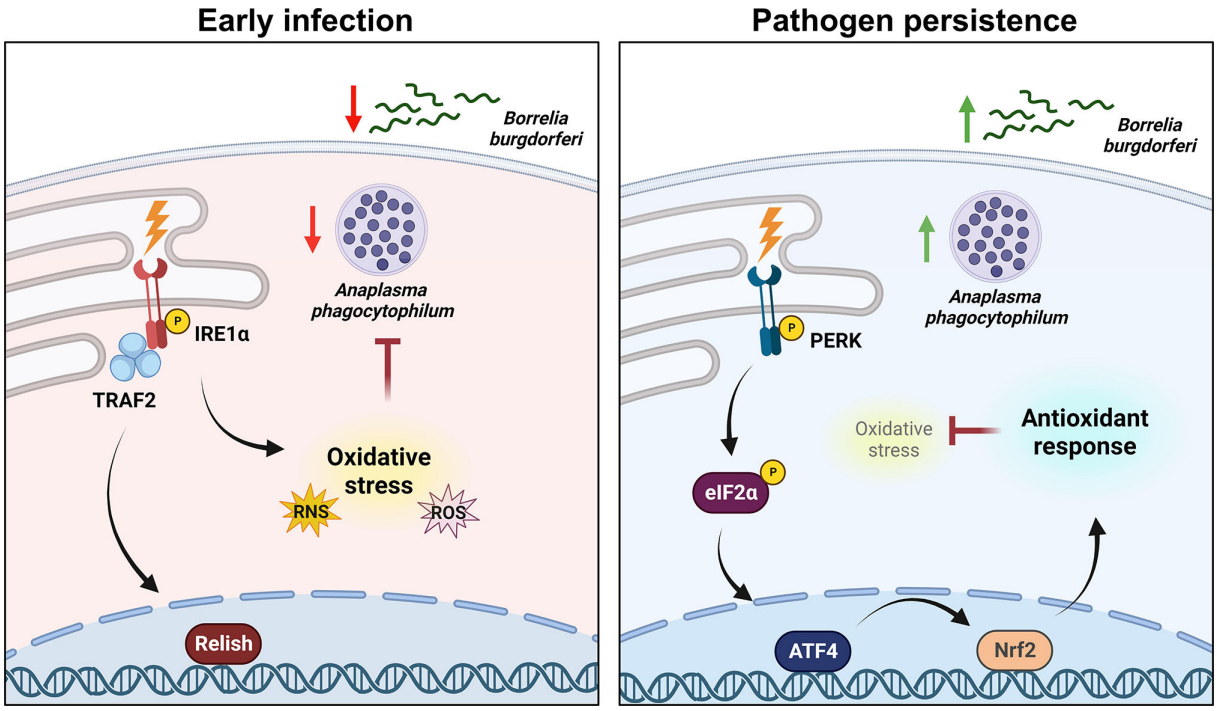


**FIG 7** The PERK-eIF2α-ATF4 axis promotes pathogen survival in ticks through an Nrf2-mediated antioxidant response. When colonizing the tick, *A. phagocytophilum* and *B. burgdorferi* trigger the *Ixodes* IMD pathway and ROS/RNS through the IRE1α-TRAF2 axis of the UPR. Tick-borne microbes persist in the tick over time by stimulating the PERK branch of the UPR, which signals through eIF2α and the transcription factors ATF4 and Nrf2 to trigger an antioxidant response that promotes microbial survival.

caused by infection (76). For example, pathogens can secrete toxic by-products, compete with the host for limiting amounts of nutrients, and/or cause physical damage to host cells (25). Our previous study demonstrated that both *Borrelia* and *Anaplasma* activate the IRE1α-TRAF2 branch of the UPR in ticks, which results in the accumulation of ROS (20). When this pathway was inhibited, ROS levels were either partially (*Anaplasma*) or completely (*Borrelia*) mitigated. Since oxidative stress is an important stimulus that triggers the UPR (77, 78), it is possible that ROS potentiated by the IRE1α-TRAF2 pathway is the signal that activates the PERK pathway at later time points and results in an antioxidant response. From this perspective, the PERK-eIF2α-ATF4-Nrf2 pathway may be a host-driven response that promotes the preservation of "self."

Unexpectedly, we observed that *A. phagocytophilum* and *B. burgdorferi* caused a decline in RNS that began either a few hours after infection (*A. phagocytophilum*) or after 2 days (*B. burgdorferi*) (Fig. 6C and D). A potential explanation for this could be increased arginase expression. Arginase competes for the nitric oxide synthase substrate L-arginine and is therefore a potent inhibitor of nitric oxide production (79). Villar et al. reported that *Ixodes arginase* expression levels are significantly increased in *A. phagocytophilum*-infected ticks (80), which could explain the rapid decline in RNS we observed after *Anaplasma* infection (Fig. 6C). Similarly, a recent report by Sapiro et al. analyzed *I. scapularis* nymphs by mass spectrometry and reported that Arginase was enriched with *B. burgdorferi* after 4 days of feeding but not at early time points (81). This may explain why RNS also decreased with *B. burgdorferi* (Fig. 6D) but only after 48 h of infection.

The Nrf2 gene regulatory network has not yet been characterized in *I. scapularis*. Mammalian Nrf2 regulates components of the glutathione and thioredoxin antioxidant systems as well as enzymes involved in NADPH regeneration (82, 83). Given that ROS levels increased in tick cells when Nrf2 was knocked down (Fig. 5F), it is reasonable to speculate that similar antioxidant genes are regulated by *Ixodes* Nrf2. Moreover, it is well established that tick-borne microbes benefit from antioxidant gene expression

in the tick (74, 84–92). For example, manipulating selenium-related antioxidant gene expression has microbicidal consequences for microbes in the tick (84–86, 89, 91, 93). This is in agreement with our findings that Nrf2 expression promotes *Borrelia* and *Anaplasma* survival (Fig. 5G and H) and further indicates that the *Ixodes* Nrf2 coordinates an antioxidant gene network.

Between human and *Ixodes* Nrf2, we observed structural conservation in the bZIP domain with 100% conservation of the amino acids that make direct contact with DNA (Fig. 5C and D). However, there was low sequence conservation (Fig. S2A), and the *Ixodes* Nrf2 is almost 400 amino acids longer than the human Nrf2. This may suggest that there are regulatory mechanisms or protein-protein interactions that are unique to the tick. In addition to protein differences, the *Ixodes* Nrf2-regulated gene network also appears to be divergent. For example, heme oxygenase is an important cytoprotective protein regulated by Nrf2 in most eukaryotes and has been implicated in disease tolerance (94). However, chelicerates do not have a gene encoding heme oxygenase (95). Altogether, this suggests that there are differences in Nrf2 and the genes it coordinates between ticks and other eukaryotes, which may be tailored to the life histories of each organism. The extent of divergence between *Ixodes* Nrf2 and other eukaryotes is a question that remains unanswered at this time.

During an infection, there are two potential immunological outcomes: (i) immune resistance, aimed at eliminating invading microbes, or (ii) tolerance to infection, where the host tolerates the presence of pathogens (96, 97). Tolerance to infection is a host defense strategy that decreases the overall impact that infection has on host health and fitness. While immune responsiveness is necessary for survival during an infection, an overly robust response can be harmful to the host by damaging tissues and depleting energy stores. Vector-borne pathogens and their arthropod hosts have long-established co-evolutionary histories (76, 98, 99). The result is a relationship balance where microbes are restricted from overwhelming the arthropod but are ultimately tolerated (76). Our findings have now shed mechanistic light on this push and pull, collectively illustrating a scenario where early tick infection triggers IREα-TRAF2 signaling leading to IMD pathway activation and ROS production (20), while persistent infection induces the PERK pathway and an antioxidant response through Nrf2 that supports pathogen survival (Fig. 7). Innate immune mediators, such as AMPs and ROS, have potent antimicrobial activity, but the non-specificity of these molecules can also cause damage to host tissues (76). We speculate that the PERK-driven antioxidant response in persistently infected ticks is a host-driven response aimed at reducing collateral damage to self. Ultimately, this network preserves tick fitness but also promotes pathogen persistence. The result is a balance between microbial restriction and host preservation that promotes arthropod tolerance to infection by transmissible pathogens.

## MATERIALS AND METHODS

### Bacteria and animal models

Roswell Park Memorial Institute 1640 medium supplemented with 10% heat-inactivated fetal bovine serum (FBS; Atlanta Biologicals, S11550) and 1× Glutamax (Gibco, 35050061) was used to culture *A. phagocytophilum* strain HZ in HL60 cells (ATCC, CCL-240) under biosafety level 2 conditions. Cultures were maintained between $1 \times 10^5$ and $1 \times 10^6$ cells/mL at 37°C in the presence of 5% $CO_2$. Mice were infected with $1 \times 10^7$ host cell free *A. phagocytophilum* in 100 µL of PBS (Intermountain Life Sciences, BSS-PBS) intraperitoneally as previously described (10, 20). Six days post-infection, 25–50 µL of infected blood was collected from the lateral saphenous vein of each mouse, and *A. phagocytophilum* burdens were assessed via quantitative PCR [*16S* relative to mouse β-actin (20, 100, 101)].

*B. burgdorferi* B31 [MSK5 (20, 102)] was grown at 37°C with 5% $CO_2$ in modified Barbour-Stoenner-Kelly II (BSK-II) medium supplemented with 6% normal rabbit serum (NRS; Pel-Freez, 31126–5) under biosafety level 2 conditions. Density and growth phase

of the spirochetes were assessed by dark-field microscopy. Prior to infection, plasmid verification was performed as previously described (20, 102). Mice were inoculated with $1 \times 10^5$ low-passage spirochetes in 100 µL of 1:1 PBS:NRS intradermally. Mice were bled from the lateral saphenous vein at 7 days post-infection. *B. burgdorferi*-infected blood (25–50 µL) was cultured in BSK-II medium and examined for the presence of spirochetes by dark-field microscopy (20, 103, 104).

Male C57BL/6 mice, aged 6–10 weeks old, obtained from colonies maintained at Washington State University were used for all experiments. Guidelines and protocols approved by the American Association for Accreditation of Laboratory Animal Care (AAALAC) and by the Office of Campus Veterinarian at Washington State University (Animal Welfare Assurance A3485-01, IACUC-approved protocol #6097) were used for all experiments utilizing mice. The animals were housed and maintained in an AAALAC-accredited facility at Washington State University in Pullman, WA. All procedures were approved by the Washington State University Biosafety and Animal Care and Use Committees.

*Ixodes scapularis* ticks at the larval stage were obtained from the Biodefense and Emerging Infectious Diseases Research Resources Repository from the National Institute of Allergy and Infectious Diseases (www.beiresources.org) at the National Institutes of Health or from Oklahoma State University (Stillwater, OK, USA). Ticks were maintained in a 23°C incubator with 16:8-h light:dark photoperiods and 95–100% relative humidity.

## Tick cell and HEK293 T cultures

*I. scapularis* embryonic cell lines ISE6 and IDE12 were cultured at 32°C with 1% $CO_2$ in L15C-300 and L15C media, respectively. These growth media were supplemented with 10% heat-inactivated FBS (Sigma, F0926), 10% tryptose phosphate broth (BD, B260300) and 0.1% lipoprotein bovine cholesterol (MP Biomedicals, 219147680) (20, 105).

HEK293 T cells were maintained in Dulbecco's modified Eagle medium (DMEM; Sigma, D6429) supplemented with 10% heat-inactivated FBS (Atlanta Biologicals, S11550) and 1× Glutamax. Cells were maintained in T75 culture flasks (Corning, 353136) at 33°C or 37°C in 5% $CO_2$.

## Pharmacological treatments and RNAi silencing

ISE6 and IDE12 cells were seeded at $1 \times 10^6$ cells per well in a 24-well plate and pre-treated with ISRIB (Cayman Chemical, 16258) or salubrinal (Thermo Scientific, AAJ64192LB0) for 1 h prior to infection. Cells were infected with *A. phagocytophilum* or *B. burgdorferi* at a multiplicity of infection (MOI) of 50 for 18 h alone or in the presence of 50-mM NAC (Sigma, A7250). Cells were collected in RIPA buffer (for immunoblotting) or TRIzol for RNA (Invitrogen, 15596026). RNA was extracted with the Direct-zol RNA Microprep Kit (Zymo, R2062), and cDNA was synthesized from 300 to 500 ng total RNA using the Verso cDNA Synthesis Kit (Thermo Fisher Scientific, AB1453B). Bacterial burden was assessed by quantitative reverse transcription PCR (qRT-PCR) with iTaq universal SYBR Green Supermix (Bio-Rad, 1725125). Cycling conditions used were as recommended by the manufacturer.

Transfection experiments used siRNAs and scrambled RNAs (scRNAs) synthesized with the Silencer siRNA Construction Kit (Invitrogen, AM1620). ISE6 or IDE12 cells were seeded at $1 \times 10^6$ cells per well in a 24-well plate or $2.5 \times 10^5$ per well in a 96-well plate. siRNA or scRNA (3 µg) in conjunction with 2.5 µL Lipofectamine 2000 (Invitrogen, 11668027) was transfected into tick cells overnight in 24-well plates. siRNA or scRNA (1 µg) with 1 µL Lipofectamine 2000 was used for 96-well plates. Cells were infected with *A. phagocytophilum* (MOI 50) or *B. burgdorferi* (MOI 50) for 18 h. Cells infected with *Anaplasma* had the cell culture supernatant removed before collecting in TRIzol. Cells infected with *Borrelia* had both cells and supernatant collected in TRIzol. RNA was isolated and transcripts were assessed by qRT-PCR as described above. All data are expressed as means ± standard error of the mean (SEM).

## Polyacrylamide gel electrophoresis and immunoblotting

Protein concentrations from cells collected in RIPA (radioimmunoprecipitation assay) buffer were quantified by bicinchoninic acid assay (Pierce, 23225). Protein (25 µg) was loaded onto a 4–15% MP TGX precast cassette (Bio-Rad, 4561083), and proteins were separated at 100 V for 1 h 25 min. Proteins were transferred to a polyvinylidene difluoride (PVDF) membrane and were blocked with 5% bovine serum albumin (BSA) in 1× tris-buffered saline containing 0.1% Tween 20 (TBS-T) for 1–2 h at room temperature. The eIF2α antibody (1:500; EMD Millipore 07–760-I) was incubated with the PVDF membrane overnight at 4°C in 5% BSA in TBS-T. On the following day, a secondary antibody was applied (donkey anti-rabbit–HRP; Thermo Fisher Scientific; A16023; 1:2,000). Blots were visualized with enhanced chemiluminescence Western blotting substrate (Thermo Fisher Scientific, 32106).

## ROS and RNS assays

ISE6 cells ($1.68 \times 10^5$) per well were seeded in a 96-well plate with black walls and clear bottoms (Thermo Scientific, 165305). All wells were treated with the fluorescent detection probes DCF-DA (10 µM; Sigma, D2926) or 4,5-diaminoflurescein diacetate (5 µM; Cayman Chemical, 85165) for 1 h in Ringer buffer (155 mM NaCl, 5 mM KCl, 1 mM $MgCl_2 \cdot 6H_2O$, 2-mM $NaH_2PO_4 \cdot H_2O$, 10 mM HEPES, and 10 mM glucose) (20, 106). Cells were treated with the probe alone or in the presence of 1 µM ISRIB. Buffer was removed and cells were washed with PBS at room temperature. *A. phagocytophilum* or *B. burgdorferi* were then added at an MOI of 50 in the presence of ISRIB or vehicle control (DMSO). Fluorescence was measured at 504 nm/529 nm at the indicated times, and data were graphed as fold change of relative fluorescence unit normalized to the negative control ±SEM.

## Luciferase reporter assay

HEK293 T cells were seeded in white-walled, clear-bottom 96-well plates (Greiner Bio-One, 655098) at a density of $1 \times 10^4$ cells per well. On the following day, cells were transfected with 0.05 µg of each vector from the UPR/ER stress response luciferase reporter vector set (Signosis, LR-3007) and 0.5 µL of Lipofectamine 2000 in Opti-MEM I reduced-serum medium (Gibco, 31985062). Transfections were allowed to proceed overnight. On the following day, the medium containing the plasmid-Lipofectamine 2,000 complex was removed and replaced with complete DMEM for an additional 18–24 h. Cells were then infected with *A. phagocytophilum* at an MOI of 50 or *B. burgdorferi* at an MOI of 200 or were left uninfected overnight. On the following day, D-luciferin potassium salt (RPI, L37060) was added to each well at a final concentration of 5 mg/mL, and luminescence was measured. Data are graphed as relative light unit normalized to uninfected controls ± SEM.

## Gene expression analysis of whole ticks

Gene expression profiling of whole ticks was performed on flat, unfed nymphs that were infected with *A. phagocytophilum* or *B. burgdorferi* as larvae. Individual ticks were snap frozen in liquid nitrogen and mechanically pulverized prior to the addition of TRIzol. RNA extraction and qRT-PCR analysis were performed as described above with primers listed in Table S1. Gene expression levels were measured by qRT-PCR and normalized to uninfected controls. Data are expressed as means ± SEM.

## RNAi silencing and analysis of whole ticks

RNAi silencing in *I. scapularis* larvae was performed as described previously (20). Briefly, approximately 150 larvae were transferred to a 1.5-mL tube with 40 µL of siRNA or scrambled controls and were incubated overnight at 15°C. Larvae were then dried

and allowed to recover overnight under normal maintenance conditions prior to being placed onto mice the following day. Larvae were allowed to feed to repletion and frozen at three time points: immediately following collection, after resting (7 days for *A. phagocytophilum*, 14 days for *B. burgdorferi*), and after molting into nymphs. Replete larvae were weighed in groups of three to assess feeding efficiency before being processed individually, as described above. qRT-PCR analysis was performed with the use of a standard curve to generate absolute numbers of the target sequences. Primers used to generate the plasmids used in the standard curves are the same as the primers used to measure target levels (Table S1), with the exception of *A. phagocytophilum 16S*.

### Protein alignments and modeling

*I. scapularis* proteins were identified using National Center for Biotechnology Information protein BLAST and querying the tick genome with human protein sequences for eIF2α (NP_004827.4) and Nrf2 (NP_001138884.1). Alignments were visualized with JalView (107). Physiochemical property conservation between amino acids is indicated by shading. AlphaFold (46, 47) was used to model the protein structure of *Ixodes* Nrf2 and align it to the human Nrf2 protein structure. Alignments were visualized with UCSF ChimeraX (48).

### Statistical analysis

*In vitro* experiments were performed with three to five replicates. *In vivo* experiments used at least 10–20 ticks. Data were expressed as means ± SEM and analyzed with either an unpaired Student's *t*-test or a non-parametric Mann-Whitney test. Calculations and graphs were created with GraphPad Prism. A $P$ value of $<0.05$ was considered statistically significant.

## ACKNOWLEDGMENTS

We are grateful to Ulrike Munderloh (University of Minnesota) for providing ISE6 and IDE12 tick cell lines, Jon Skare (Texas A&M Health Science Center) for providing *B. burgdorferi* B31 (MSK5), Biodefense and Emerging Infectious Diseases Resources and Oklahoma State University for *Ixodes scapularis* ticks, and Arden Baylink (Washington State University) for guidance with AlphaFold and UCSF ChimeraX. Schematics in Fig. 1 and 7 were created with Biorender.com.

This work is supported by the National Institutes of Health (R21AI148578, R21AI139772, and R01AI162819 to D.K.S.), the WSU Intramural CVM grants program, funded in part by the National Institute of Food and Agriculture, and the Joseph and Barbara Mendelson Endowment Research Fund (to D.K.S.) and Washington State University, College of Veterinary Medicine. J.H. and K.A.V. are trainees supported by an Institutional T32 Training Grant from the National Institute of Allergy and Infectious Diseases (T32GM008336). E.A.F. is a trainee supported by an Institutional T32 Training Grant from the National Institute of Allergy and Infectious Diseases (T32AI007025). Additional support to L.C.S.-L. came from The Fowler Emerging Diseases Graduate Fellowship funded by Ralph and Maree Fowler, the Kraft Graduate Scholarship, and the Poncin Fellowship. E.R.-Z. is a trainee supported by an Institutional Training Grant MIRA R25 ESTEEMED from the National Institute of Biomedical Imaging and Bioengineering (R25EB027606). The content is solely the responsibility of the authors and does not necessarily represent the official views of the National Institute of Allergy and Infection Diseases or the National Institutes of Health.

K.L.R., J.H., and D.K.S. designed the study. K.L.R., J.H., E.A.F., K.A.V., A.L.W., L.C.S.-L., S.J.W., E.R.-Z., J.M.P., and D.K.S. contributed to methodology, investigation, and data analysis. All authors provided intellectual input into the study. K.L.R. and D.K.S. wrote the manuscript. All authors contributed to editing.

## AUTHOR AFFILIATIONS

[1]Department of Veterinary Microbiology and Pathology, Washington State University, Pullman, Washington, USA
[2]School of Molecular Biosciences, Washington State University, Pullman, Washington, USA

## PRESENT ADDRESS

Joanna Hurtado, Entrogen, Inc, Woodland Hills, California, USA

## AUTHOR ORCIDs

Jason M. Park http://orcid.org/0000-0002-9050-5277
Dana K. Shaw http://orcid.org/0000-0002-5212-2494



## FUNDING

| Funder | Grant(s) | Author(s) |
|---|---|---|
| HHS \| NIH \| National Institute of Allergy and Infectious Diseases (NIAID) | R21AI148578, R21AI139772, R01AI162819 | Dana K. Shaw |
| HHS \| NIH \| National Institute of Allergy and Infectious Diseases (NIAID) | T32GM008336 | Joanna Hurtado |
| HHS \| NIH \| National Institute of Allergy and Infectious Diseases (NIAID) | T32GM008336 | Kaylee A. Vosbigian |
| HHS \| NIH \| National Institute of Allergy and Infectious Diseases (NIAID) | T32AI007025 | Elis A. Fisk |
| HHS \| NIH \| National Institute of Biomedical Imaging and Bioengineering (NIBIB) | R25EB027606 | Elisabeth Ramirez-Zepp |


## AUTHOR CONTRIBUTIONS

Kristin L. Rosche, Conceptualization, Data curation, Formal analysis, Investigation, Methodology, Writing – original draft, Writing – review and editing | Joanna Hurtado, Conceptualization, Data curation, Formal analysis, Investigation, Methodology | Elis A. Fisk, Data curation, Investigation, Methodology, Writing – review and editing | Kaylee A. Vosbigian, Data curation, Formal analysis, Investigation, Methodology, Writing – review and editing | Ashley L. Warren, Data curation, Formal analysis, Investigation, Methodology | Lindsay C. Sidak-Loftis, Data curation, Investigation, Methodology | Sarah J. Wright, Data curation, Investigation, Methodology, Writing – review and editing | Elisabeth Ramirez-Zepp, Data curation, Methodology | Jason M. Park, Data curation, Writing – review and editing | Dana K. Shaw, Conceptualization, Data curation, Formal analysis, Funding acquisition, Investigation, Methodology, Project administration, Resources, Supervision, Validation, Writing – original draft, Writing – review and editing

## ADDITIONAL FILES

The following material is available online.

### Supplemental Material

**Supplemental figure legends (mSphere00321-23-s0001.docx).** Legends for Figures S1-S4.
**Figure S1 (mSphere00321-23-s0002.tif).** Sequence alignment of eIF2α from *I. scapularis* and *Homo sapiens*.
**Figure S2 (mSphere00321-23-s0003.tif).** *Ixodes* Nrf2 sequence alignment and structural prediction with AlphaFold.

**Figure S3 (mSphere00321-23-s0004.tif).** ISRIB does not potentiate ROS or RNS in tick cells.
**Figure S4 (mSphere00321-23-s0005.tif).** Exogenous N-acetyl cysteine reduces the ROS caused by silencing PERK.
**Table S1 (mSphere00321-23-s0006.pdf).** Oligonucleotide primers used in this study.

## REFERENCES


1. WHO. n.d. Vector-borne diseases. WHO. Available from: http://www.who.int/mediacentre/factsheets/fs387/en
2. Paddock CD, Lane RS, Staples JE, Labruna MB. 2016. Changing paradigms for tick-borne diseases in the Americas. In Global health impacts of vector-borne diseases: workshop summary. National Academies Press (US), Washington (DC).
3. 2011. "The short-term and long-term outcomes: workshop report" Critical Needs and Gaps in Understanding Prevention, Amelioration, and Resolution of Lyme and Other Tick-Borne Diseases; National Academies Press, Washington, D.C. https://doi.org/10.17226/13134
4. Jongejan F, Uilenberg G. 2004. The global importance of ticks. Parasitology 129 Suppl:S3–S14. https://doi.org/10.1017/-s0031182004005967
5. Park JM, Oliva Chávez AS, Shaw DK. 2021. Ticks: more than just a pathogen delivery service. Front Cell Infect Microbiol 11:739419. https://doi.org/10.3389/fcimb.2021.739419
6. Adegoke A, Ribeiro JMC, Brown S, Smith RC, Karim S. 2023. *Rickettsia parkeri* hijacks tick hemocytes to manipulate cellular and humoral transcriptional responses. Front Immunol 14:1094326. https://doi.org/10.3389/fimmu.2023.1094326
7. Liu L, Narasimhan S, Dai J, Zhang L, Cheng G, Fikrig E. 2011. *Ixodes scapularis* salivary gland protein P11 facilitates migration of *Anaplasma phagocytophilum* from the tick gut to salivary glands. EMBO Rep 12:1196–1203. https://doi.org/10.1038/embor.2011.177
8. Johns R, Ohnishi J, Broadwater A, Sonenshine DE, De Silva AM, Hynes WL. 2001. Contrasts in tick innate immune responses to *Borrelia burgdorferi* challenge: immunotolerance in *Ixodes scapularis* versus immunocompetence in *Dermacentor variabilis* (acari: ixodidae). J Med Entomol 38:99–107. https://doi.org/10.1603/0022-2585-38.1.99
9. Rittig MG, Kuhn K-H, Dechant CA, Gauckler A, Modolell M, Ricciardi-Castagnoli P, Krause A, Burmester GR. 1996. Phagocytes from both vertebrate and invertebrate species use "coiling" phagocytosis. Dev Comp Immunol 20:393–406. https://doi.org/10.1016/s0145-305x(96)00023-7
10. Shaw DK, Wang X, Brown LJ, Chávez ASO, Reif KE, Smith AA, Scott AJ, McClure EE, Boradia VM, Hammond HL, Sundberg EJ, Snyder GA, Liu L, DePonte K, Villar M, Ueti MW, de la Fuente J, Ernst RK, Pal U, Fikrig E, Pedra JHF. 2017. Infection-derived lipids elicit an immune deficiency circuit in arthropods. Nat Commun 8:14401. https://doi.org/10.1038/ncomms14401
11. McClure Carroll EE, Wang X, Shaw DK, O'Neal AJ, Oliva Chávez AS, Brown LJ, Boradia VM, Hammond HL, Pedra JHF. 2019. P47 licenses activation of the immune deficiency pathway in the tick *Ixodes scapularis*. Proc Natl Acad Sci U S A 116:205–210. https://doi.org/10.1073/pnas.1808905116
12. Rosa RD, Capelli-Peixoto J, Mesquita RD, Kalil SP, Pohl PC, Braz GR, Fogaça AC, Daffre S. 2016. Exploring the immune signalling pathway-related genes of the cattle tick *Rhipicephalus microplus*: from molecular characterization to transcriptional profile upon microbial challenge. Dev Comp Immunol 59:1–14. https://doi.org/10.1016/j.dci.2015.12.018
13. Smith A. A., Pal U. 2014. Immunity-related genes in *Ixodes scapularis*--perspectives from genome information. Front Cell Infect Microbiol 4:116. https://doi.org/10.3389/fcimb.2014.00116
14. Liu L, Dai J, Zhao YO, Narasimhan S, Yang Y, Zhang L, Fikrig E. 2012. *Ixodes scapularis* JAK-STAT pathway regulates tick antimicrobial peptides, thereby controlling the agent of human granulocytic anaplasmosis. J Infect Dis 206:1233–1241. https://doi.org/10.1093/infdis/jis484
15. Smith AA, Navasa N, Yang X, Wilder CN, Buyuktanir O, Marques A, Anguita J, Pal U. 2016. Cross-species interferon signaling boosts microbicidal activity within the tick vector. Cell Host Microbe 20:91–98. https://doi.org/10.1016/j.chom.2016.06.001
16. Rana VS, Kitsou C, Dutta S, Ronzetti MH, Zhang M, Bernard Q, Smith AA, Tomás-Cortázar J, Yang X, Wu M-J, Kepple O, Li W, Dwyer JE, Matias J, Baljinnyam B, Oliver JD, Rajeevan N, Pedra JHF, Narasimhan S, Wang Y, Munderloh U, Fikrig E, Simeonov A, Anguita J, Pal U. 2023. Dome1–JAK–STAT signaling between parasite and host integrates vector immunity and development. Science 379:eabl3837. https://doi.org/10.1126/science.abl3837
17. O'Neal AJ, Singh N, Rolandelli A, Laukaitis HJ, Wang X, Shaw DK, Young BD, Narasimhan S, Dutta S, Snyder GA, Samaddar S, Marnin L, Butler LR, Mendes MT, Cabrera Paz FE, Valencia LM, Sundberg EJ, Fikrig E, Pal U, Weber DJ, Pedra JHF. 2023. Croquemort elicits activation of the immune deficiency pathway in ticks. Proc Natl Acad Sci U S A 120:e2208673120. https://doi.org/10.1073/pnas.2208673120
18. Gulia-Nuss M, Nuss AB, Meyer JM, Sonenshine DE, Roe RM, Waterhouse RM, Sattelle DB, de la Fuente J, Ribeiro JM, Megy K, Thimmapuram J, Miller JR, Walenz BP, Koren S, Hostetler JB, Thiagarajan M, Joardar VS, Hannick LI, Bidwell S, Hammond MP, Young S, Zeng Q, Abrudan JL, Almeida FC, Ayllón N, Bhide K, Bissinger BW, Bonzon-Kulichenko E, Buckingham SD, Caffrey DR, Caimano MJ, Croset V, Driscoll T, Gilbert D, Gillespie JJ, Giraldo-Calderón GI, Grabowski JM, Jiang D, Khalil SMS, Kim D, Kocan KM, Koči J, Kuhn RJ, Kurtti TJ, Lees K, Lang EG, Kennedy RC, Kwon H, Perera R, Qi Y, Radolf JD, Sakamoto JM, Sánchez-Gracia A, Severo MS, Silverman N, Šimo L, Tojo M, Tornador C, Van Zee JP, Vázquez J, Vieira FG, Villar M, Wespiser AR, Yang Y, Zhu J, Arensburger P, Pietrantonio PV, Barker SC, Shao R, Zdobnov EM, Hauser F, Grimmelikhuijzen CJP, Park Y, Rozas J, Benton R, Pedra JHF, Nelson DR, Unger MF, Tubio JMC, Tu Z, Robertson HM, Shumway M, Sutton G, Wortman JR, Lawson D, Wikel SK, Nene VM, Fraser CM, Collins FH, Birren B, Nelson KE, Caler E, Hill CA. 2016. Genomic insights into the *Ixodes scapularis* tick vector of lyme disease. Nat Commun 7:10507. https://doi.org/10.1038/ncomms10507
19. Palmer WJ, Jiggins FM. 2015. Comparative genomics reveals the oigins and diversity of arthropod immune systems. Mol Biol Evol 32:2111–2129. https://doi.org/10.1093/molbev/msv093
20. Sidak-Loftis LC, Rosche KL, Pence N, Ujczo JK, Hurtado J, Fisk EA, Goodman AG, Noh SM, Peters JW, Shaw DK. 2022. The unfolded-protein response triggers the arthropod immune deficiency pathway mBio 13:e0292222. https://doi.org/10.1128/mbio.02922-22
21. Rosche KL, Sidak-Loftis LC, Hurtado J, Fisk EA, Shaw DK. 2020. Arthropods under pressure: stress responses and immunity at the pathogen-vector interface. Front Immunol 11:629777. https://doi.org/10.3389/fimmu.2020.629777
22. Grootjans J, Kaser A, Kaufman RJ, Blumberg RS. 2016. The unfolded protein response in immunity and inflammation. Nat Rev Immunol 16:469–484. https://doi.org/10.1038/nri.2016.62
23. Hetz C. 2012. The unfolded protein response: controlling cell fate decisions under ER stress and beyond. Nat Rev Mol Cell Biol 13:89–102. https://doi.org/10.1038/nrm3270
24. Schröder M, Kaufman RJ. 2005. The mammalian unfolded protein response. Annu Rev Biochem 74:739–789. https://doi.org/10.1146/annurev.biochem.73.011303.074134
25. Casadevall A, Pirofski L. 2001. Host - pathogen interactions: the attributes of virulence. J Infect Dis 184:337–344. https://doi.org/10.1086/322044
26. Pakos-Zebrucka K, Koryga I, Mnich K, Ljujic M, Samali A, Gorman AM. 2016. The integrated stress response. EMBO Rep. 17:1374–1395. https://doi.org/10.15252/embr.201642195
27. Harding HP, Zhang Y, Zeng H, Novoa I, Lu PD, Calfon M, Sadri N, Yun C, Popko B, Paules R, Stojdl DF, Bell JC, Hettmann T, Leiden JM, Ron D. 2003. An integrated stress response regulates amino acid metabolism

and resistance to oxidative stress. Mol Cell 11:619–633. https://doi.org/10.1016/s1097-2765(03)00105-9
28. Taniuchi S, Miyake M, Tsugawa K, Oyadomari M, Oyadomari S. 2016. Integrated stress response of vertebrates is regulated by four eIF2α kinases. Sci Rep 6:32886. https://doi.org/10.1038/srep32886
29. Donnelly N, Gorman AM, Gupta S, Samali A. 2013. The eIF2α kinases: their structures and functions. Cell Mol Life Sci 70:3493–3511. https://doi.org/10.1007/s00018-012-1252-6
30. Ohoka N, Yoshii S, Hattori T, Onozaki K, Hayashi H. 2005. TRB3, a novel ER stress-inducible gene, is induced via ATF4–CHOP pathway and is involved in cell death. EMBO J. 24:1243–1255. https://doi.org/10.1038/sj.emboj.7600596
31. Han J, Back SH, Hur J, Lin Y-H, Gildersleeve R, Shan J, Yuan CL, Krokowski D, Wang S, Hatzoglou M, Kilberg MS, Sartor MA, Kaufman RJ. 2013. ER-stress-induced transcriptional regulation increases protein synthesis leading to cell death. Nat Cell Biol 15:481–490. https://doi.org/10.1038/ncb2738
32. Sidrauski C, McGeachy AM, Ingolia NT, Walter P. 2015. The small molecule ISRIB reverses the effects of eIF2α phosphorylation on translation and stress granule assembly. Elife 4:e05033. https://doi.org/10.7554/eLife.05033
33. Long K, Boyce M, Lin H, Yuan J, Ma D. 2005. Structure–activity relationship studies of salubrinal lead to its active biotinylated derivative. Bioorg Med Chem Lett 15:3849–3852. https://doi.org/10.1016/j.bmcl.2005.05.120
34. Boyce M, Bryant KF, Jousse C, Long K, Harding HP, Scheuner D, Kaufman RJ, Ma D, Coen DM, Ron D, Yuan J. 2005. A selective inhibitor of eIF2α dephosphorylation protects cells from ER stress. Science 307:935–939. https://doi.org/10.1126/science.1101902
35. Hodzic E, Fish D, Maretzki CM, De Silva AM, Feng S, Barthold SW. 1998. Acquisition and transmission of the agent of human granulocytic ehrlichiosis by *Ixodes scapularis* ticks. J Clin Microbiol 36:3574–3578. https://doi.org/10.1128/JCM.36.12.3574-3578.1998
36. Abraham NM, Liu L, Jutras BL, Yadav AK, Narasimhan S, Gopalakrishnan V, Ansari JM, Jefferson KK, Cava F, Jacobs-Wagner C, Fikrig E. 2017. Pathogen-mediated manipulation of arthropod microbiota to promote infection. Proc Natl Acad Sci U S A 114:E781–E790. https://doi.org/10.1073/pnas.1613422114
37. Narasimhan S, Rajeevan N, Liu L, Zhao YO, Heisig J, Pan J, Eppler-Epstein R, Deponte K, Fish D, Fikrig E. 2014. Gut microbiota of the tick vector *Ixodes scapularis* modulate colonization of the lyme disease spirochete. Cell Host Microbe 15:58–71. https://doi.org/10.1016/j.chom.2013.12.001
38. Narasimhan S, Schuijt TJ, Abraham NM, Rajeevan N, Coumou J, Graham M, Robson A, Wu M-J, Daffre S, Hovius JW, Fikrig E. 2017. Modulation of the tick gut milieu by a secreted tick protein favors *Borrelia burgdorferi* colonization. Nat Commun 8:184. https://doi.org/10.1038/s41467-017-00208-0
39. Piesman J, Oliver JR, Sinsky RJ. 1990. Growth kinetics of the lyme disease spirochete (*Borrelia burgdorferi*) in vector ticks (*Ixodes dammini*). Am J Trop Med Hyg 42:352–357. https://doi.org/10.4269/ajtmh.1990.42.352
40. Pal U, Kitsou C, Drecktrah D, Yaş ÖB, Fikrig E. 2021. Interactions between ticks and lyme disease spirochetes. Curr Issues Mol Biol 42:113–144. https://doi.org/10.21775/cimb.042.113
41. Anderson JM, Sonenshine DE, Valenzuela JG. 2008. Exploring the mialome of ticks: an annotated catalogue of midgut transcripts from the hard tick, *Dermacentor variabilis* (acari: ixodidae). BMC Genomics 9:552. https://doi.org/10.1186/1471-2164-9-552
42. Ebnet K, Brown KD, Siebenlist UK, Simon MM, Shaw S. 1997. Borrelia burgdorferi activates nuclear factor-kappa β and is a potent inducer of chemokine and adhesion molecule gene expression in endothelial cells and fibroblasts. J Immunol 158:3285–3292.
43. Lee HC, Kioi M, Han J, Puri RK, Goodman JL. 2008. *Anaplasma phagocytophilum*-induced gene expression in both human neutrophils and HL-60 cells. Genomics 92:144–151. https://doi.org/10.1016/j.ygeno.2008.05.005
44. Dumler JS, Lichay M, Chen W-H, Rennoll-Bankert KE, Park J-H. 2020. *Anaplasma phagocytophilum* activates NF-κβ signaling via redundant pathways. Front Public Health 8:558283. https://doi.org/10.3389/fpubh.2020.558283
45. Sarkar A, Hellberg L, Bhattacharyya A, Behnen M, Wang K, Lord JM, Möller S, Kohler M, Solbach W, Laskay T. 2012. Infection with *Anaplasma phagocytophilum* activates the phosphatidylinositol 3-kinase/akt and NF-κβ survival pathways in neutrophil granulocytes. Infect Immun 80:1615–1623. https://doi.org/p10.1128/IAI.05219-11
46. Jumper J, Evans R, Pritzel A, Green T, Figurnov M, Ronneberger O, Tunyasuvunakool K, Bates R, Žídek A, Potapenko A, Bridgland A, Meyer C, Kohl SAA, Ballard AJ, Cowie A, Romera-Paredes B, Nikolov S, Jain R, Adler J, Back T, Petersen S, Reiman D, Clancy E, Zielinski M, Steinegger M, Pacholska M, Berghammer T, Bodenstein S, Silver D, Vinyals O, Senior AW, Kavukcuoglu K, Kohli P, Hassabis D. 2021. Highly accurate protein structure prediction with AlphaFold. Nature 596:583–589. https://doi.org/10.1038/s41586-021-03819-2
47. Varadi M, Anyango S, Deshpande M, Nair S, Natassia C, Yordanova G, Yuan D, Stroe O, Wood G, Laydon A, Žídek A, Green T, Tunyasuvunakool K, Petersen S, Jumper J, Clancy E, Green R, Vora A, Lutfi M, Figurnov M, Cowie A, Hobbs N, Kohli P, Kleywegt G, Birney E, Hassabis D, Velankar S. 2022. AlphaFold protein structure database: massively expanding the structural coverage of protein-sequence space with high-accuracy models. Nucleic Acids Res. 50:D439–D444. https://doi.org/10.1093/nar/gkab1061
48. Pettersen EF, Goddard TD, Huang CC, Meng EC, Couch GS, Croll TI, Morris JH, Ferrin TE. 2021. UCSF ChimeraX: structure visualization for researchers, educators, and developers. Protein Sci. 30:70–82. https://doi.org/10.1002/pro.3943
49. Moi P, Chan K, Asunis I, Cao A, Kan YW. 1994. Isolation of NF-E2-related factor 2 (Nrf2), a NF-E2-like basic leucine zipper transcriptional activator that binds to the tandem NF-E2/AP1 repeat of the beta-globin locus control region. Proc Natl Acad Sci U S A 91:9926–9930. https://doi.org/10.1073/pnas.91.21.9926
50. Hayes JD, Dinkova-Kostova AT. 2014. The Nrf2 regulatory network provides an interface between redox and intermediary metabolism. Trends Biochem Sci 39:199–218. https://doi.org/10.1016/j.tibs.2014.02.002
51. Sarcinelli C, Dragic H, Piecyk M, Barbet V, Duret C, Barthelaix A, Ferraro-Peyret C, Fauvre J, Renno T, Chaveroux C, Manié SN. 2020. ATF4-dependent NRF2 transcriptional regulation promotes antioxidant protection during endoplasmic reticulum stress. Cancers (Basel) 12:569. https://doi.org/10.3390/cancers12030569
52. Cullinan SB, Diehl JA. 2004. PERK-dependent activation of Nrf2 contributes to redox homeostasis and cell survival following endoplasmic reticulum stress. J Biol Chem 279:20108–20117. https://doi.org/10.1074/jbc.M314219200
53. He CH, Gong P, Hu B, Stewart D, Choi ME, Choi AM, Alam J. 2001. Identification of activating transcription factor 4 (ATF4) as an Nrf2-interacting protein: IMPLICATION FOR HEME OXYGENASE-1 GENE REGULATION. J Biol Chem 276:20858–20865. https://doi.org/10.1074/jbc.M101198200
54. Itoh K, Chiba T, Takahashi S, Ishii T, Igarashi K, Katoh Y, Oyake T, Hayashi N, Satoh K, Hatayama I, Yamamoto M, Nabeshima Y. 1997. An Nrf2/small maf heterodimer mediates the induction of phase II detoxifying enzyme genes through antioxidant response elements. Biochem Biophys Res Commun 236:313–322. https://doi.org/10.1006/bbrc.1997.6943
55. Rushmore TH, Morton MR, Pickett CB. 1991. The antioxidant responsive element. activation by oxidative stress and identification of the DNA consensus sequence required for functional activity. J Biol Chem 266:11632–11639.
56. De S, Kingan SB, Kitsou C, Portik DM, Foor SD, Frederick JC, Rana VS, Paulat NS, Ray DA, Wang Y, Glenn TC, Pal U. 2023. A high-quality *Ixodes scapularis* genome advances tick science. Nat Genet 55:301–311. https://doi.org/10.1038/s41588-022-01275-w
57. Sengoku T, Shiina M, Suzuki K, Hamada K, Sato K, Uchiyama A, Kobayashi S, Oguni A, Itaya H, Kasahara K, Moriwaki H, Watanabe C, Honma T, Okada C, Baba S, Ohta T, Motohashi H, Yamamoto M, Ogata K. 2022. Structural basis of transcription regulation by CNC family transcription factor, Nrf2. Nucleic Acids Res. 50:12543–12557. https://doi.org/10.1093/nar/gkac1102
58. Lin M, Rikihisa Y. 2007. Degradation of p22phox and inhibition of superoxide generation by *Ehrlichia chaffeensis* in human monocytes. Cell Microbiol 9:861–874. https://doi.org/10.1111/j.1462-5822.2006.00835.x

59. Boylan JA, Gherardini FC. 2008. Determining the cellular targets of reactive oxygen species in *Borrelia burgdorferi*. Methods Mol Biol 431:213–221. https://doi.org/10.1007/978-1-60327-032-8_17
60. Hyde JA, Shaw DK, Smith Iii R, Trzeciakowski JP, Skare JT. 2009. The BosR regulatory protein of *Borrelia burgdorferi* interfaces with the RpoS regulatory pathway and modulates both the oxidative stress response and pathogenic properties of the Lyme disease spirochete. Mol Microbiol 74:1344–1355. https://doi.org/10.1111/j.1365-2958.2009.06951.x
61. Hyde JA, Shaw DK, Smith R, Trzeciakowski JP, Skare JT. 2010. Characterization of a conditional bosR mutant in *Borrelia burgdorferi*. Infect Immun 78:265–274. https://doi.org/10.1128/IAI.01018-09
62. Mott J, Rikihisa Y. 2000. Human granulocytic ehrlichiosis agent inhibits superoxide anion generation by human neutrophils. Infect Immun 68:6697–6703. https://doi.org/10.1128/IAI.68.12.6697-6703.2000
63. Carlyon JA, Fikrig E. 2003. Invasion and survival strategies of *Anaplasma phagocytophilum*. Cell Microbiol 5:743–754. https://doi.org/10.1046/j.1462-5822.2003.00323.x
64. Carlyon JA, Abdel-Latif D, Pypaert M, Lacy P, Fikrig E. 2004. *Anaplasma phagocytophilum* utilizes multiple host evasion mechanisms to thwart NADPH oxidase-mediated killing during neutrophil infection. Infect Immun 72:4772–4783. https://doi.org/10.1128/IAI.72.8.4772-4783.2004
65. Alberdi P, Cabezas-Cruz A, Prados PE, Rayo MV, Artigas-Jerónimo S, de la Fuente J. 2019. The redox metabolic pathways function to limit *Anaplasma phagocytophilum* infection and multiplication while preserving fitness in tick vector cells. Sci Rep 9:13236. https://doi.org/10.1038/s41598-019-49766-x
66. Boylan JA, Lawrence KA, Downey JS, Gherardini FC. 2008. *Borrelia burgdorferi* membranes are the primary targets of reactive oxygen species. Mol Microbiol 68:786–799. https://doi.org/10.1111/j.1365-2958.2008.06204.x
67. Ramsey ME, Hyde JA, Medina-Perez DN, Lin T, Gao L, Lundt ME, Li X, Norris SJ, Skare JT, Hu LT. 2017. A high-throughput genetic screen identifies previously uncharacterized *Borrelia burgdorferi* genes important for resistance against reactive oxygen and nitrogen species. PLOS Pathog. 13:e1006225. https://doi.org/10.1371/journal.ppat.1006225
68. Bourret TJ, Lawrence KA, Shaw JA, Lin T, Norris SJ, Gherardini FC. 2016. The nucleotide excision repair pathway protects *Borrelia burgdorferi* from nitrosative stress in *Ixodes scapularis* ticks. Front Microbiol 7:1397. https://doi.org/10.3389/fmicb.2016.01397
69. Bourret TJ, Boylan JA, Lawrence KA, Gherardini FC. 2011. Nitrosative damage to free and zinc-bound cysteine thiols underlies nitric oxide toxicity in wild-type *Borrelia burgdorferi*. Mol Microbiol 81:259–273. https://doi.org/10.1111/j.1365-2958.2011.07691.x
70. Troxell B, Zhang J-J, Bourret TJ, Zeng MY, Blum J, Gherardini F, Hassan HM, Yang XF. 2014. Pyruvate protects pathogenic spirochetes from $H_2O_2$ killing. PLoS One 9:e84625. https://doi.org/10.1371/journal.pone.0084625
71. Yang X, Smith AA, Williams MS, Pal U. 2014. A dityrosine network mediated by dual oxidase and peroxidase influences the persistence of lyme disease pathogens within the vector. J Biol Chem 289:12813–12822. https://doi.org/10.1074/jbc.M113.538272
72. Ma Y, Seiler KP, Tai KF, Yang L, Woods M, Weis JJ. 1994. Outer surface lipoproteins of *Borrelia burgdorferi* stimulate nitric oxide production by the cytokine-inducible pathway. Infect Immun 62:3663–3671. https://doi.org/10.1128/iai.62.9.3663-3671.1994
73. Modolell M, Schaible UE, Rittig M, Simon MM. 1994. Killing of *Borrelia burgdorferi* by macrophages is dependent on oxygen radicals and nitric oxide and can be enhanced by antibodies to outer surface proteins of the spirochete. Immunol Lett 40:139–146. https://doi.org/10.1016/0165-2478(94)90185-6
74. Narasimhan S, Sukumaran B, Bozdogan U, Thomas V, Liang X, DePonte K, Marcantonio N, Koski RA, Anderson JF, Kantor F, Fikrig E. 2007. A tick antioxidant facilitates the lyme disease agent's successful migration from the mammalian host to the arthropod vector. Cell Host Microbe 2:7–18. https://doi.org/10.1016/j.chom.2007.06.001
75. Park JM, Genera BM, Fahy D, Swallow KT, Nelson CM, Oliver JD, Shaw DK, Munderloh UG, Brayton KA. 2023. An *Anaplasma phagocytophilum* T4SS effector, AteA, is essential for tick infection. bioRxiv:2023.02.06.527355. https://doi.org/10.1101/2023.02.06.527355
76. Shaw DK, Tate AT, Schneider DS, Levashina EA, Kagan JC, Pal U, Fikrig E, Pedra JHF. 2018. Vector immunity and evolutionary ecology: the harmonious dissonance. Trends Immunol. 39:862–873. https://doi.org/10.1016/j.it.2018.09.003
77. Ding W, Yang L, Zhang M, Gu Y. 2012. Reactive oxygen species-mediated endoplasmic reticulum stress contributes to aldosterone-induced apoptosis in tubular epithelial cells. Biochem Biophys Res Commun 418:451–456. https://doi.org/10.1016/j.bbrc.2012.01.037
78. Liu Z-W, Zhu H-T, Chen K-L, Dong X, Wei J, Qiu C, Xue J-H. 2013. Protein kinase RNA- like endoplasmic reticulum kinase (PERK) signaling pathway plays a major role in reactive oxygen species (ROS)- mediated endoplasmic reticulum stress- induced apoptosis in diabetic cardiomyopathy. Cardiovasc Diabetol 12:158. https://doi.org/10.1186/1475-2840-12-158
79. Durante W, Johnson FK, Johnson RA. 2007. Arginase: a critical regulator of nitric oxide synthesis and vascular function. Clin Exp Pharmacol Physiol 34:906–911. https://doi.org/10.1111/j.1440-1681.2007.04638.x
80. Villar M, Ayllón N, Alberdi P, Moreno A, Moreno M, Tobes R, Mateos-Hernández L, Weisheit S, Bell-Sakyi L, de la Fuente J. 2015. Integrated metabolomics, transcriptomics and proteomics identifies metabolic pathways affected by *Anaplasma phagocytophilum* infection in tick cells. Mol Cell Proteomics 14:3154–3172. https://doi.org/10.1074/mcp.M115.051938
81. Sapiro AL, Hayes BM, Volk RF, Zhang JY, Brooks DM, Martyn C, Radkov A, Zhao Z, Kinnersley M, Secor PR, Zaro BW, Chou S. 2023. Longitudinal map of transcriptome changes in the lyme pathogen *Borrelia burgdorferi* during tick-borne transmission. Elife 12:RP86636. https://doi.org/10.7554/eLife.86636
82. Tonelli C, Chio IIC, Tuveson DA. 2018. Transcriptional regulation by Nrf2. Antioxid Redox Signal 29:1727–1745. https://doi.org/10.1089/ars.2017.7342
83. Gorrini C, Harris IS, Mak TW. 2013. Modulation of oxidative stress as an anticancer strategy. Nat Rev Drug Discov 12:931–947. https://doi.org/10.1038/nrd4002
84. Budachetri K, Karim S. 2015. An insight into the functional role of thioredoxin reductase, a selenoprotein, in maintaining normal native microbiota in the gulf-coast tick (*Amblyomma maculatum*). Insect Mol Biol 24:570–581. https://doi.org/10.1111/imb.12184
85. Budachetri K, Kumar D, Karim S. 2017. Catalase is a determinant of the colonization and transovarial transmission of *Rickettsia parkeri* in the gulf coast tick *Amblyomma maculatum* . Insect Mol Biol 26:414–419. https://doi.org/10.1111/imb.12304
86. Kumar D, Embers M, Mather TN, Karim S. 2019. Is selenoprotein K required for Borrelia burgdorferi infection within the tick vector *Ixodes scapularis*?. Parasit Vectors 12:289. https://doi.org/10.1186/s13071-019-3548-y
87. Hernandez EP, Talactac MR, Vitor RJS, Yoshii K, Tanaka T. 2021. An *Ixodes scapularis* glutathione S-transferase plays a role in cell survival and viability during langat virus infection of a tick cell line. Acta Trop 214:105763. https://doi.org/10.1016/j.actatropica.2020.105763
88. Crispell G, Budachetri K, Karim S. 2016. *Rickettsia parkeri* colonization in *Amblyomma maculatum*: the role of superoxide dismutases. Parasit Vectors 9:291. https://doi.org/10.1186/s13071-016-1579-1
89. Adamson SW, Browning RE, Budachetri K, Ribeiro JMC, Karim S, Munderloh UG. 2013. Knockdown of selenocysteine-specific elongation factor in *Amblyomma maculatum* alters the pathogen burden of *Rickettsia parkeri* with epigenetic control by the sin3 histone deacetylase corepressor complex. PLOS ONE 8:e82012. https://doi.org/10.1371/journal.pone.0082012
90. Kocan KM, Zivkovic Z, Blouin EF, Naranjo V, Almazán C, Mitra R, de la Fuente J. 2009. Silencing of genes involved in *Anaplasma marginale*-tick interactions affects the pathogen developmental cycle in *Dermacentor variabilis*. BMC Dev Biol 9:42. https://doi.org/10.1186/1471-213X-9-42
91. Kumar D, Budachetri K, Meyers VC, Karim S. 2016. Assessment of tick antioxidant responses to exogenous oxidative stressors and insight into the role of catalase in the reproductive fitness of the gulf coast tick, *Amblyomma Maculatum*. Insect Mol Biol 25:283–294. https://doi.org/10.1111/imb.12218
92. Kalil SP, Rosa R da, Capelli-Peixoto J, Pohl PC, Oliveira P de, Fogaça AC, Daffre S. 2017. Immune-related redox metabolism of embryonic cells of the tick *Rhipicephalus microplus* (BME26) in response to infection with

*Anaplasma marginale*. Parasit Vectors 10:613. https://doi.org/10.1186/s13071-017-2575-9
93. Budachetri K, Kumar D, Crispell G, Beck C, Dasch G, Karim S. 2018. The tick endosymbiont *Candidatus midichloria mitochondrii* and selenoproteins are essential for the growth of *Rickettsia parkeri* in the gulf coast tick vector. Microbiome 6:141. https://doi.org/10.1186/s40168-018-0524-2
94. DeSouza-Vieira T, Iniguez E, Serafim TD, de Castro W, Karmakar S, Disotuar MM, Cecilio P, Lacsina JR, Meneses C, Nagata BM, Cardoso S, Sonenshine DE, Moore IN, Borges VM, Dey R, Soares MP, Nakhasi HL, Oliveira F, Valenzuela JG, Kamhawi S. 2020. Heme oxygenase-1 induction by blood-feeding arthropods controls skin inflammation and promotes disease tolerance. Cell Reports 33:108317. https://doi.org/10.1016/j.celrep.2020.108317
95. Perner J, Sobotka R, Sima R, Konvickova J, Sojka D, Oliveira PL de, Hajdusek O, Kopacek P. n.d. Acquisition of exogenous Haem is essential for tick reproduction. eLife 5:e12318. https://doi.org/10.7554/eLife.12318
96. Medzhitov R, Schneider DS, Soares MP. 2012. Disease tolerance as a defense strategy. Science 335:936–941. https://doi.org/10.1126/science.1214935
97. Ayres JS, Schneider DS. 2012. Tolerance of infections. Annu Rev Immunol 30:271–294. https://doi.org/10.1146/annurev-immunol-020711-075030
98. Estrada-Peña A, Álvarez-Jarreta J, Cabezas-Cruz A. 2018. Reservoir and vector evolutionary pressures shaped the adaptation of *Borrelia*. Infect Genet Evol 66:308–318. https://doi.org/10.1016/j.meegid.2018.03.023
99. Powell JR. 2019. An evolutionary perspective on vector-borne diseases. Front Genet 10:1266. https://doi.org/10.3389/fgene.2019.01266
100. Sukumaran B, Ogura Y, Pedra JHF, Kobayashi KS, Flavell RA, Fikrig E. 2012. Rip2 contributes to host defense against *Anaplasma phagocytophilum* infection. FEMS Immunol Med Microbiol 66:211–219. https://doi.org/10.1111/j.1574-695X.2012.01001.x
101. Pedra JHF, Sutterwala FS, Sukumaran B, Ogura Y, Qian F, Montgomery RR, Flavell RA, Fikrig E. 2007. ASC/PYCARD and caspase-1 regulate the IL-18/IFN-γ axis during *Anaplasma phagocytophilum* infection1. J Immunol 179:4783–4791. https://doi.org/10.4049/jimmunol.179.7.4783
102. Labandeira-Rey M, Skare JT. 2001. Decreased infectivity in *Borrelia burgdorferi* strain B31 is associated with loss of linear Plasmid 25 or 28-1. Infect Immun 69:446–455. https://doi.org/10.1128/IAI.69.1.446-455.2001
103. James AE, Rogovskyy AS, Crowley MA, Bankhead T. 2016. Characterization of a DNA Adenine methyltransferase gene of *Borrelia hermsii* and its dispensability for murine infection and persistence. PLOS ONE 11:e0155798. https://doi.org/10.1371/journal.pone.0155798
104. Bankhead T, Chaconas G. 2007. The role of VlsE antigenic variation in the lyme disease spirochete: persistence through a mechanism that differs from other pathogens. Mol Microbiol 65:1547–1558. https://doi.org/10.1111/j.1365-2958.2007.05895.x
105. Severo MS, Choy A, Stephens KD, Sakhon OS, Chen G, Chung D-WD, Le Roch KG, Blaha G, Pedra JHF. 2013. The E3 ubiquitin ligase XIAP restricts *Anaplasma phagocytophilum* colonization of *Ixodes scapularis* ticks. J Infect Dis 208:1830–1840. https://doi.org/10.1093/infdis/jit380
106. Abuaita BH, Schultz TL, O'Riordan MX. 2018. Mitochondria-derived vesicles deliver antimicrobial reactive oxygen species to control phagosome-localized *Staphylococcus aureus*. Cell Host Microbe 24:625–636. https://doi.org/10.1016/j.chom.2018.10.005
107. Waterhouse AM, Procter JB, Martin DMA, Clamp M, Barton GJ. 2009. Jalview version 2—a multiple sequence alignment editor and analysis workbench. Bioinformatics 25:1189–1191. https://doi.org/10.1093/bioinformatics/btp033